

Late-time Background Constraints on Linear and Non-linear Interacting Dark Energy after DESI DR2

David Figueruelo,^{1, 2, *} Marcel van der Westhuizen,^{3, †} Amare Abebe,^{3, 4, ‡} and Eleonora Di Valentino^{5, §}

¹*Department of Theoretical Physics, University of the Basque Country UPV/EHU, 48080 Bilbao, Spain*

²*Institute of Theoretical Astrophysics, University of Oslo, N-0315 Oslo, Norway*

³*Centre for Space Research, North-West University, Potchefstroom 2520, South Africa*

⁴*National Institute for Theoretical and Computational Sciences (NITheCS), South Africa*

⁵*School of Mathematical and Physical Sciences, University of Sheffield,
Hounsfield Road, Sheffield S3 7RH, United Kingdom*

In this study, we present observational constraints on a class of phenomenological interacting dark energy (IDE) models that admit analytical solutions for the Hubble parameter $H(z)$. We consider a set of five linear and three non-linear IDE scenarios, encompassing both interactions proportional to the dark matter and/or dark energy densities, as well as non-linear combinations of the two. For all eight IDE models, we find a better fit than Λ CDM from a $\Delta\chi^2$ analysis for both combinations of datasets considered. When using the Akaike Information Criterion (ΔAIC), we find a similarly improved fit in all cases, except for one dataset combination in $Q = 3H\delta\rho_{\text{de}}$. Our analysis also shows a preference for sign-switching interactions, with energy transfer from dark energy to dark matter at low redshift, reversing direction at higher redshift. These results should be interpreted with caution, as the latter direction of energy transfer is accompanied by negative dark energy densities in the past, which may be unphysical. Models that do not allow sign-changing behaviour instead show a preference for energy flow from dark matter to dark energy, and hence negative dark energy densities. The only exceptions are $Q = 3H\delta\rho_{\text{de}}$ and $Q = 3H\delta\left(\frac{\rho_{\text{de}}^2}{\rho_{\text{dm}} + \rho_{\text{de}}}\right)$, which exhibit energy flow in the opposite direction. Furthermore, for all interactions considered, we find a phantom-divide crossing in the effective dark energy equation of state $w_{\text{de}}^{\text{eff}}$, with the dark energy density decreasing ($w_{\text{de}}^{\text{eff}} > -1$) at present and at low redshift, while increasing ($w_{\text{de}}^{\text{eff}} < -1$) in the past at high redshift. These results highlight the promising, but problematic, nature of dark sector interactions, as well as the need to extend the analysis using early-time physics and datasets.

I. INTRODUCTION

Cosmology has entered a new era driven by an unprecedented wealth of observational data collected in recent years. This change has reshaped the way cosmology itself develops as a science, since any new proposal must now be evaluated against the plethora of available datasets. Large galaxy surveys such as DESI [1, 2] or DES [3], extraordinarily precise measurements of the Cosmic Microwave Background from Planck [4], and Supernovae light curve observations [5, 6], among many others, have elevated cosmology to a discipline built upon exquisite and precise observations. The diversity of these measurements has provided us with a map of the Universe across different epochs and scales, while allowing us to test and rule out alternative models with a level of precision unimaginable just a few decades ago. These data have established the Λ Cold Dark Matter model (Λ CDM) as the standard cosmological model, yet they have also highlighted its most profound mystery: the required dominance of a dark sector. This dark sector, however, comes with its own theoretical challenges [7–10]. At the frontier of modern cosmology lies this dark sector, a realm whose elusive nature continues to challenge our deepest attempts to unveil the fundamental laws of the Universe.

In addition to this mystery, we have reached a point where such an abundance of precise data has led to the emergence of tensions in cosmological measurements [11–25], with the Hubble H_0 tension being of extraordinary concern and the S_8 tension of comparatively lesser significance. One possible explanation for these discrepancies is their origin in observational systematics or miscalibrations; however, as data quality improves and additional datasets become available, this possibility is increasingly disfavoured [26–29]. If systematics are not the cause, these tensions are rendered more pressing by the *trend* they exhibit: values inferred from early-Universe experiments, where Λ CDM is deeply embedded in the analysis, versus values obtained from late-time measurements that rely far less on the Λ CDM framework, rather than by the nominal statistical significance (in σ) separating the two measurements. This point is not inconsequential but rather pivotal if we are to truly understand the current situation. It therefore raises

* david.figueruelo@ehu.eus

† marcelvdw007@gmail.com

‡ amare.abebe@nithecs.ac.za

§ e.divalentino@sheffield.ac.uk

a central question: to what extent are these tensions the result of a potential incompleteness of the Λ CDM model? In addition to these long-standing cosmological tensions, the recent DESI data [1, 2] have introduced a possible new discrepancy by suggesting a preference for dynamical dark energy, although this issue remains under active debate. Within this context, the study of alternatives to the reference Λ CDM model is well motivated: first, as a means of better understanding the standard model itself, and second, as a pathway toward potentially improved descriptions of our Universe.

The landscape of modifications to the Λ CDM model is as vast as our imagination allows, but it can be broadly summarised as follows: modifications or reformulations of gravity [30–51], dynamical dark energy [1, 52–104], the introduction of new species [105–112], non-gravitational interactions involving the dark sector [113–152], modifications at recombination [153–161], and Early Dark Energy or other early-time solutions [15, 162–181]. Although the idea of dark sector interactions was originally proposed to address the coincidence problem, such interactions have more recently been put forward as potential explanations for the aforementioned cosmological tensions.

In this study, we focus on the specific case of a non-gravitational energy transfer within the dark sector, broadly known as Interacting Dark Energy (IDE) models. Here, we restrict our analysis to the background evolution, leaving the study of perturbations for future work. This paper should therefore be understood as a continuation of Refs. [150–152]. As previously mentioned, these models were introduced shortly after the discovery of the accelerated expansion of the Universe to address the coincidence problem [182–193]. The coincidence problem arises from the different dilution rates of the dark components: the cosmological constant does not dilute ($\rho_\Lambda = \text{constant}$), while dark matter dilutes proportionally to the expansion of the Universe ($\rho_{\text{dm}} \propto a^{-3}$). Despite this striking difference in dilution rates, observers in our Universe appear to live at a particular epoch in which both components are of the same order of magnitude. The distant past and future correspond to entirely different scenarios, which naturally raises the question: why now? Following their initial introduction, IDE models experienced a resurgence in popularity driven by the persistent nature of the aforementioned cosmological tensions and the search for possible extensions to the Λ CDM model. In particular, the potential of IDE models to address the H_0 tension has been explored extensively [13, 119, 120, 122, 126, 132, 133, 135–137, 141–146, 148, 149, 173, 194–196], while the impact of interacting dark sectors on the S_8 tension has been studied in [115, 117, 140, 197–204]. More recently, claims of a possible dynamical nature of dark energy emerging from the DESI DR2¹ data release [1, 52, 205, 206] have prompted renewed interest in models capable of simultaneously providing a dynamical description of dark energy and allowing for a phantom crossing. This has led to further investigations of IDE models as viable candidates to address key problems in cosmology [97, 148, 207–217]. Other approaches aimed at explaining the DESI DR2 results can be found in [66, 218–220].

Our study builds upon these investigations by specifically constraining a set of phenomenological IDE models using the same BAO data from DESI DR2, together with cosmological data from Pantheon+, Cosmic Clocks, and BBN. The models considered here have recently been studied in [150–152], where new analytical solutions for the Hubble function were derived, along with conditions describing the occurrence of negative energy densities and future singularities. This work can therefore be regarded as the first set of observational constraints on these models using the most up-to-date data following these theoretical developments, enabling us to draw new conclusions regarding a possible preference in cosmological data for negative energy densities within the framework of IDE models.

This paper is structured as follows. In Section II, we introduce the interacting dark energy models considered in this work and describe their theoretical framework. In Section III, we present the datasets and methodology used in our analysis, together with the resulting observational constraints. Finally, we summarize our main conclusions and outline future prospects in Section IV.

II. INTERACTING DARK ENERGY MODELS

In this section, we introduce the models considered in this work and present the equations that govern their dynamics. For detailed discussions of the models and the derivation of the equations presented here, we refer the reader to Refs. [150–152], where the theoretical analyses are carried out in full.

Throughout this work, we assume that the different components of the Universe can be described as perfect fluids. Accordingly, we associate with each component an energy density ρ_i , a pressure p_i , and a four-velocity u_i^μ . We also assign to each component a stress-energy tensor $T_i^{\mu\nu}$, which is covariantly conserved for each individual, non-interacting component, $\nabla_\mu T_i^{\mu\nu} = 0$. However, for the interacting dark energy and dark matter components considered here, the conservation equations take the form

$$\nabla_\mu T_{\text{de}}^{\mu\nu} = -\nabla_\mu T_{\text{dm}}^{\mu\nu} = Q^\nu. \quad (1)$$

¹ Similar results were previously reported in the DESI DR1 data release [53].

Here, Q^ν denotes the interaction four-vector and represents the flow of energy between the two dark sectors. Since we are only interested in the background evolution, we do not require the full four-vector Q^ν , but only its background zeroth component, which we denote simply by Q . In this paper, we consider a variety of interacting models in which the coupling kernel Q is proportional, either linearly or non-linearly, to the dark sector densities. The dynamics of these models are governed by the modified conservation equation (1), which at the background level leads to the following set of conservation equations:

$$\dot{\rho}_{\text{dm}} + 3H\rho_{\text{dm}} = Q, \quad \dot{\rho}_{\text{de}} + 3H\rho_{\text{de}}(1+w) = -Q. \quad (2)$$

Here, the overdot denotes differentiation with respect to cosmic time, ρ_{dm} and ρ_{de} are the energy densities of dark matter and dark energy, respectively, H is the Hubble function, and w is the dark energy equation-of-state parameter. Dark matter is assumed to be pressureless. From these equations, it is clear that $Q > 0$ corresponds to an energy transfer from dark energy to dark matter, while $Q < 0$ describes energy flow from dark matter to dark energy. The direction of this energy exchange can significantly affect both the background dynamics and the expansion history of the Universe. Assuming that all other parameters are kept fixed to their Λ CDM values and that only the interaction is introduced, we expect the following deviations from standard cosmology:

1. **Energy flow from dark energy to dark matter:** This scenario leads to less dark matter and more dark energy in the past, thereby *alleviating the coincidence problem*. The suppression of the dark matter density results in a lower value of H_0 at late times, thus *worsening the H_0 tension*. In addition, the matter power spectrum is suppressed with respect to late-time probes, which *alleviates the S_8 tension* [200]. Energy flow in this direction also *increases the age of the Universe* and tends to *avoid both negative energy densities and future big rip singularities* [150, 151], while remaining consistent with the laws of thermodynamics [221].
2. **Energy flow from dark matter to dark energy:** Energy transfer in this direction generally produces the opposite effects to those described above. Nevertheless, it is often considered attractive due to its potential to alleviate the Hubble tension, as demonstrated in [113–149, 152, 222–229].

It should be emphasized that many of the consequences outlined above hold only if all cosmological parameters are kept fixed. Once other parameters, such as $\Omega_{\text{dm},0}$, H_0 , and w , are allowed to vary freely, different conclusions may be reached depending on their inferred posterior distributions. Another important consideration is that some interactions exhibit a sign-switching behaviour, which can lead to combinations of the consequences described above.

II.1. Linear models

In this analysis, we consider five interaction kernels proportional in a linear manner to either the dark matter or dark energy density, or a combination of both. The background dynamics of these interactions were recently studied in [150]. Specifically, we consider the general interaction given by the kernel $Q = 3H(\delta_{\text{dm}}\rho_{\text{dm}} + \delta_{\text{de}}\rho_{\text{de}})$ and four of its special cases.

$$\text{Linear IDE model 1: } Q = 3H(\delta_{\text{dm}}\rho_{\text{dm}} + \delta_{\text{de}}\rho_{\text{de}})$$

For a flat FLRW universe containing radiation, baryons, dark matter, and dark energy, this interaction has the normalized Hubble function found in Ref. [152]:

$$E(z) = \left\{ -\frac{1}{2\Delta} \left[\Omega_{(\text{de},0)} (\delta_{\text{dm}} - \delta_{\text{de}} + w - \Delta) + \Omega_{(\text{dm},0)} (\delta_{\text{dm}} - \delta_{\text{de}} - w - \Delta) \right] (1+z)^{-\frac{3}{2}(\delta_{\text{dm}} - \delta_{\text{de}} - w - 2 + \Delta)} \right. \\ \left. + \frac{1}{2\Delta} \left[\Omega_{(\text{de},0)} (\delta_{\text{dm}} - \delta_{\text{de}} + w + \Delta) + \Omega_{(\text{dm},0)} (\delta_{\text{dm}} - \delta_{\text{de}} - w + \Delta) \right] (1+z)^{-\frac{3}{2}(\delta_{\text{dm}} - \delta_{\text{de}} - w - 2 - \Delta)} \right. \\ \left. + \Omega_{\text{bm},0}(1+z)^3 + \Omega_{\text{r},0}(1+z)^4 \right\}^{\frac{1}{2}}, \quad (3)$$

where $\Omega_{(\text{dm},0)}$ and $\Omega_{(\text{de},0)}$ are the present ($z = 0$) density parameters for dark matter and dark energy, δ_{dm} and δ_{de} are dimensionless coupling constants that determine how strongly the interaction is coupled to dark matter and dark

energy, respectively, while w is the dark energy equation of state. We also assume that both baryonic matter and dark matter have no pressure. Notably, the determinant Δ appears and is given by:

$$\Delta = \sqrt{(\delta_{\text{dm}} + \delta_{\text{de}} + w)^2 - 4\delta_{\text{de}}\delta_{\text{dm}}} . \quad (4)$$

The sign of δ_{dm} determines the initial direction of energy transfer, while δ_{de} determines the late-time energy transfer. In both cases, a positive coupling implies energy transfer from dark energy to dark matter, and vice versa for a negative coupling. This implies that if δ_{dm} and δ_{de} have opposite signs, the direction of energy transfer will change at some point during the cosmological evolution. Furthermore, $\delta_{\text{dm}} < 0$ leads to negative dark energy in the past, while $\delta_{\text{de}} < 0$ predicts negative dark matter in the future, as shown in [150].

$$\text{Linear IDE model 2: } Q = 3H\delta(\rho_{\text{dm}} + \rho_{\text{de}})$$

The Hubble function for this model is given by (3) when we set $\delta_{\text{dm}} = \delta_{\text{de}} = \delta$. This model exhibits negative dark energy densities in the past and negative dark matter densities in the future if energy flows from dark matter to dark energy (given by $\delta < 0$), while all energy densities remain positive if there is a small interaction from dark energy to dark matter (given by $\delta > 0$), provided the conditions in Table II are satisfied.

Previous observational constraints for this model may be found in [216, 226, 228, 230–238].

$$\text{Linear IDE model 3: } Q = 3H\delta(\rho_{\text{dm}} - \rho_{\text{de}})$$

The Hubble function for this model is given by (3) when we set $\delta_{\text{dm}} = \delta$ and $\delta_{\text{de}} = -\delta$. This is a sign-switching interaction, with the sign of δ determining the initial direction of energy transfer. If $\delta < 0$, the energy initially flows from dark matter to dark energy and reverses at some point during the evolution. This behaviour is also accompanied by negative dark energy densities in the past. In contrast, if $\delta > 0$, the initial energy flow is from dark energy to dark matter, which later changes to energy transfer from dark matter to dark energy. This scenario further predicts that dark matter becomes negative in the future.

Previous observational constraints for this model may be found in [119, 237, 239].

$$\text{Linear IDE model 4: } Q = 3H\delta\rho_{\text{dm}}$$

The Hubble function for this model is given by (3) when we set $\delta_{\text{dm}} = \delta$ and $\delta_{\text{de}} = 0$. If energy flows from dark matter to dark energy (given by $\delta < 0$), this interaction leads to negative dark energy densities in the past, while all energy densities remain positive for a small interaction from dark energy to dark matter (given by $\delta > 0$).

Previous observational constraints for this model may be found in [13, 113, 120, 141, 216, 230–234, 237, 238, 240–247].

$$\text{Linear IDE model 5: } Q = 3H\delta\rho_{\text{de}}$$

The Hubble function for this model is given by (3) when we set $\delta_{\text{de}} = \delta$ and $\delta_{\text{dm}} = 0$. If energy flows from dark matter to dark energy (given by $\delta < 0$), this interaction predicts negative dark matter densities in the future, while all energy densities remain positive for a small interaction from dark energy to dark matter (given by $\delta > 0$).

Previous observational constraints for this model may be found in [13, 115–117, 119, 129, 132, 133, 140, 141, 194, 196–198, 200, 201, 211, 216, 222, 230–233, 237, 240, 242–246, 248–252].

II.2. Non-linear models

In this section, we present three models in which the interaction depends on some product of the dark matter and dark energy densities, whose background dynamics were recently studied in depth in [151]. The three models discussed below can be seen as special cases of $Q = 3H\delta\left(\frac{\rho_{\text{dm}}^\alpha\rho_{\text{de}}^\beta}{\rho_{\text{dm}} + \rho_{\text{de}}}\right)$, with $(\alpha, \beta) = (1, 1)$, $(\alpha, \beta) = (2, 0)$, and $(\alpha, \beta) = (0, 2)$ corresponding to non-linear IDE models 1, 2, and 3, respectively.

$$\text{Non-linear IDE model 1: } Q = 3H\delta \left(\frac{\rho_{dm}\rho_{de}}{\rho_{dm}+\rho_{de}} \right)$$

The normalized Hubble function for this model is found in [152, 253] and is given by:

$$E(z) = \left\{ \left[\Omega_{(dm,0)}(1+z)^{3(1-\delta)} + \Omega_{(de,0)}(1+z)^{3(1+w)} \right] \left[\frac{1 + \left(\frac{\Omega_{(dm,0)}}{\Omega_{(de,0)}} \right) (1+z)^{-3(w+\delta)}}{1 + \left(\frac{\Omega_{(dm,0)}}{\Omega_{(de,0)}} \right)} \right]^{-\frac{\delta}{w+\delta}} \right. \right. \\ \left. \left. + \Omega_{bm,0}(1+z)^3 + \Omega_{r,0}(1+z)^4 \right\}^{\frac{1}{2}}. \right. \quad (5)$$

This interaction is guaranteed to always yield positive energy densities, regardless of the sign or magnitude of the interaction parameter δ .

Previous observational constraints for this model may be found in [210, 237, 245, 250, 253, 254].

$$\text{Non-linear IDE model 2: } Q = 3H\delta \left(\frac{\rho_{dm}^2}{\rho_{dm}+\rho_{de}} \right)$$

The normalized Hubble function for this model is found in [152] and is given by:

$$E(z) = \left\{ \left[\Omega_{(dm,0)} + \Omega_{(de,0)} \left(\frac{\left[w + \delta \left(\frac{\Omega_{(dm,0)}}{\Omega_{(de,0)}} \right) \right] (1+z)^{3w} - \delta \left(\frac{\Omega_{(dm,0)}}{\Omega_{(de,0)}} \right)}{w} \right) \right] (1+z)^{3\left(1-\frac{w\delta}{w-\delta}\right)} \right. \\ \left. \times \left[\frac{\left[w + \delta \left(\frac{\Omega_{(dm,0)}}{\Omega_{(de,0)}} \right) \right] (1+z)^{3w} + \left(\frac{\Omega_{(dm,0)}}{\Omega_{(de,0)}} \right) (w-\delta)}{w \left[1 + \frac{\Omega_{(dm,0)}}{\Omega_{(de,0)}} \right]} \right]^{\frac{\delta}{w-\delta}} + \Omega_{bm,0}(1+z)^3 + \Omega_{r,0}(1+z)^4 \right\}^{\frac{1}{2}}. \quad (6)$$

If energy flows from dark matter to dark energy (given by $\delta < 0$), this interaction leads to negative dark energy densities in the past, while all energy densities remain positive for a small interaction from dark energy to dark matter (given by $\delta > 0$).

Previous observational constraints for this model may be found in [237, 245, 253].

$$\text{Non-linear IDE model 3: } Q = 3H\delta \left(\frac{\rho_{de}^2}{\rho_{dm}+\rho_{de}} \right)$$

The normalized Hubble function for this model is found in [152] and is given by:

$$E(z) = \left\{ \left[\Omega_{(dm,0)} \left(\frac{\left[w \left(\frac{\Omega_{(dm,0)}}{\Omega_{(de,0)}} \right) + \delta \right] (1+z)^{-3w} - \delta}{w \left(\frac{\Omega_{(dm,0)}}{\Omega_{(de,0)}} \right)} \right) + \Omega_{(de,0)} \right] (1+z)^{3\left(1+\frac{w^2}{w-\delta}\right)} \right. \\ \left. \times \left[\frac{\left[w \left(\frac{\Omega_{(dm,0)}}{\Omega_{(de,0)}} \right) + \delta \right] (1+z)^{-3w} + w - \delta}{w \left(1 + \frac{\Omega_{(dm,0)}}{\Omega_{(de,0)}} \right)} \right]^{\frac{\delta}{w-\delta}} + \Omega_{bm,0}(1+z)^3 + \Omega_{r,0}(1+z)^4 \right\}^{\frac{1}{2}}. \quad (7)$$

If energy flows from dark matter to dark energy (given by $\delta < 0$), this interaction predicts negative dark matter densities in the future, while all energy densities remain positive for a small interaction from dark energy to dark matter (given by $\delta > 0$).

Previous observational constraints for this model may be found in [237, 245, 253, 255].

II.3. Theoretical constraints on the models

The eight interaction kernels introduced in the previous section may lead to imaginary and/or undefined energy densities for either dark matter or dark energy. The conditions required to avoid such pathological situations are

summarized in Table I. Similarly, these models may exhibit negative dark matter or dark energy densities in the past or future, as well as possible future big rip singularities, if the conditions listed in Table II are not satisfied. It is worth noting that for seven of the eight interactions studied here, negative energy densities are an inevitable consequence of energy flow from dark matter to dark energy. Predictions of future negative energy densities and future singularities are less problematic than negative energy densities in the past, since we have no observational data probing the future expansion of the Universe, and such features may simply signal a breakdown of the model beyond its domain of applicability. In contrast, the presence of negative energy densities in the past represents a more serious issue, as it would violate several energy conditions of general relativity, including the Weak Energy Condition (WEC). For discussions on the violation of energy conditions, see [256–259], while discussions on the possibility of negative dark energy, and how this may be useful in addressing recent problems in cosmology, can be found in [260–271].

Interaction Q	Conditions to avoid imaginary $\rho_{\text{dm/de}}$	Conditions to avoid undefined $\rho_{\text{dm/de}}$
$3H(\delta_{\text{dm}}\rho_{\text{dm}} + \delta_{\text{de}}\rho_{\text{de}})$	$(\delta_{\text{dm}} + \delta_{\text{de}} + w)^2 > 4\delta_{\text{de}}\delta_{\text{dm}}$	$w \neq 0 ; (\delta_{\text{dm}} + \delta_{\text{de}} + w)^2 - 4\delta_{\text{de}}\delta_{\text{dm}} \neq 0$
$3H\delta(\rho_{\text{dm}} + \rho_{\text{de}})$	$\delta \leq -\frac{w}{4}$	$w \neq 0 ; \delta \neq -\frac{w}{4}$
$3H\delta(\rho_{\text{dm}} - \rho_{\text{de}})$	$\rho_{\text{dm/de}} \text{ always real}$	$w \neq 0$
$3H\delta\rho_{\text{dm}}$	$\rho_{\text{dm/de}} \text{ always real}$	$\delta \neq -w$
$3H\delta\rho_{\text{de}}$	$\rho_{\text{dm/de}} \text{ always real}$	$\delta \neq -w$
$3H\delta\left(\frac{\rho_{\text{dm}}\rho_{\text{de}}}{\rho_{\text{dm}} + \rho_{\text{de}}}\right)$	$\rho_{\text{dm/de}} \text{ always real}$	$\delta \neq -w$
$3H\delta\left(\frac{\rho_{\text{dm}}^2}{\rho_{\text{dm}} + \rho_{\text{de}}}\right)$	$\rho_{\text{dm/de}} \text{ always real}$	$w < 0 ; w < \delta \leq -\frac{w}{r_0}$
$3H\delta\left(\frac{\rho_{\text{de}}^2}{\rho_{\text{dm}} + \rho_{\text{de}}}\right)$	$\rho_{\text{dm/de}} \text{ always real}$	$w < 0 ; w < \delta \leq -wr_0$

TABLE I. Conditions required to avoid imaginary or undefined energy densities for the different interaction kernels, as derived in [150, 151]. Here, we define $r_0 = \left(\frac{\Omega_{(\text{dm},0)}}{\Omega_{(\text{de},0)}}\right)$.

Interaction Q	$\rho_{\text{dm/de}} > 0$ domain	$\rho_{\text{dm/de}} > 0$ conditions	No future big rip
$3H(\delta_{\text{dm}}\rho_{\text{dm}} + \delta_{\text{de}}\rho_{\text{de}})$	DE \rightarrow DM	$\delta_{\text{dm}} \geq 0 ; \delta_{\text{de}} \geq 0 ; \delta_{\text{dm}}r_0 + \delta_{\text{de}} \leq -\frac{wr_0}{(1+r_0)}$	$\delta_{\text{dm}}(w+1) - \delta_{\text{de}} \leq w+1$
$3H\delta(\rho_{\text{dm}} + \rho_{\text{de}})$	DE \rightarrow DM	$0 \leq \delta \leq -\frac{wr_0}{(1+r_0)^2}$	$\delta \geq 1 + \frac{1}{w}$
$3H\delta(\rho_{\text{dm}} - \rho_{\text{de}})$	No viable domain	No viable domain	$\delta \leq \frac{1+w}{2+w}$
$3H\delta\rho_{\text{dm}}$	DE \rightarrow DM	$0 \leq \delta \leq -\frac{w}{(1+r_0)}$	$w > -1$
$3H\delta\rho_{\text{de}}$	DE \rightarrow DM	$0 \leq \delta \leq -\frac{w}{(1+\frac{1}{r_0})}$	$\delta \geq -w-1$
$3H\delta\left(\frac{\rho_{\text{dm}}\rho_{\text{de}}}{\rho_{\text{dm}} + \rho_{\text{de}}}\right)$	DE \leftrightarrow DM	$\forall \delta$	$w \geq -1$
$3H\delta\left(\frac{\rho_{\text{dm}}^2}{\rho_{\text{dm}} + \rho_{\text{de}}}\right)$	DE \rightarrow DM	$0 \leq \delta \leq -\frac{w}{r_0}$	$w \geq -1$
$3H\delta\left(\frac{\rho_{\text{de}}^2}{\rho_{\text{dm}} + \rho_{\text{de}}}\right)$	DE \rightarrow DM	$0 \leq \delta \leq -wr_0$	$\delta \geq w(w+1)$

TABLE II. Conditions required to ensure positive energy densities and avoid future big rip singularities for the different interaction kernels. Here, $r_0 = \left(\frac{\Omega_{(\text{dm},0)}}{\Omega_{(\text{de},0)}}\right)$. These conditions are derived in [150, 151].

An additional well-known pathology associated with interacting dark energy models is the presence of non-adiabatic instabilities in the dark energy perturbation equations. The standard treatment of this issue is to consider the doom factor \mathbf{d} proposed in [272], whose sign determines the presence of early-time instabilities:

$$\mathbf{d} = \frac{Q}{3H\rho_{\text{de}}(1+w)} \quad ; \quad \text{if } \begin{cases} \mathbf{d} > 1 & \rightarrow \text{Unstable runaway regime} \\ \mathbf{d} < 0 & \rightarrow \text{a priori free of instabilities} \end{cases} \quad (8)$$

Additionally, it has been pointed out that $w = -1$ causes gravitational instabilities [129, 200]. From these considerations, the standard approach is to identify two stable regimes in which Q and $(1+w)$ have opposite signs, i.e. energy flow from dark energy to dark matter ($Q > 0$) together with $w < -1$, or energy flow from dark matter to dark energy ($Q < 0$) together with $w > -1$ (see Refs. [122, 124, 136, 200, 201, 222, 234, 273]). This situation is further complicated by the fact that, for seven of the eight models considered here, we additionally find $\rho_{\text{de}} < 0$ at early times when energy flows from dark matter to dark energy ($Q < 0$) [152]. Assuming that Eq. (8) remains valid in the presence of negative dark energy, we instead require energy flow from dark matter to dark energy ($Q < 0$ and $\rho_{\text{de}} < 0$)

to be combined with a phantom dark energy equation of state, $w < -1$, in order to obtain $\mathbf{d} < 0$. We summarize how the stability of our models can be inferred from the posterior distributions in Table VIII.

The arguments presented above represent only one approach used in the literature. Another approach that has gained popularity in recent years involves treating perturbations within the Parametrized Post-Friedmann framework [240, 274–280], which is expected to open up the full parameter space. As this remains an active area of research (see [281] for recent discussions), and since the validity of using (8) when $\rho_{\text{de}} < 0$ requires further investigation, we consider our conclusions regarding the stability of our models to be preliminary. A future work, in which we will address these issues and provide explicit perturbation equations for each of the eight models discussed here, is currently in preparation. This will allow us to perform more in-depth constraints on these models, including CMB data.

Finally, for this study we do not impose artificial constraints on the parameter space to ensure positive energy densities or stability. Instead, we allow the parameters to explore the full space, find their preferred values, and then interpret the implications of the resulting constraints for each model. The only constraints we apply are those listed in Table III, which are imposed to avoid undefined energy densities, as summarized in Table I, and which could otherwise cause the MCMC runs to fail. Our approach corresponds to the *iw*CDM regime outlined in Section 4 of [152], where alternative approaches for setting priors that avoid the aforementioned theoretical pathologies are also discussed. As an example, recent constraints on the same linear interactions studied here—but with the direction of energy flow and the sign of $(1 + w)$ chosen to ensure stability—can be found in [231]. Additionally, recent constraints on three of the linear models considered here, in which the dark matter equation of state is allowed to vary ($w_{\text{dm}} \neq 0$), are presented in [216].

II.4. Phantom-crossing, effective equations of state $w_{\text{dm}}^{\text{eff}}$, $w_{\text{de}}^{\text{eff}}$ and the reconstructed equation of state \tilde{w}

A topic of recent interest is whether alternatives to the Λ CDM model may allow the dark energy equation of state w to cross the phantom divide $w = -1$ at some point in the past. This behaviour was hinted at for simple Chevallier–Polarski–Linder (CPL) parametrizations of dark energy, characterized by the parameters w_0 and w_a , by the DESI collaboration. In particular, DESI results suggest $w > -1$ at low redshift and $w < -1$ at higher redshift [52]. For the interacting dark energy models considered here, we assume the dark energy equation of state w to be constant; however, the effects of the energy exchange may still be captured through alternative descriptions.

A commonly adopted approach is to introduce effective equations of state for both dark matter, $w_{\text{dm}}^{\text{eff}}(z)$, and dark energy, $w_{\text{de}}^{\text{eff}}(z)$. This parametrization treats the system as if no interaction were present, while the evolution of each dark component is instead fully described by a redshift-dependent equation of state. The expressions for $w_{\text{dm}}^{\text{eff}}(z)$ and $w_{\text{de}}^{\text{eff}}(z)$ are obtained directly from the conservation equations (2) as:

$$w_{\text{dm}}^{\text{eff}} = -\frac{Q}{3H\rho_{\text{dm}}} \quad \text{and} \quad w_{\text{de}}^{\text{eff}} = w_{\text{de}} + \frac{Q}{3H\rho_{\text{de}}}. \quad (9)$$

Intuitively, one can note that ρ_{de} decreases when $w_{\text{de}}^{\text{eff}} > -1$ (the quintessence regime), while ρ_{de} increases when $w_{\text{de}}^{\text{eff}} < -1$ (the phantom regime).

Another approach is to introduce the reconstructed dark energy equation of state $\tilde{w}(z)$, which can be obtained from the normalized Hubble parameter $E(z)$ in a flat universe in the absence of interactions in the dark sector, such that:

$$E^2(z) = \Omega_{(\text{r},0)}(1+z)^4 + \Omega_{(\text{bm},0)}(1+z)^3 + \Omega_{(\text{dm},0)}(1+z)^3 + \Omega_{(\text{de},0)} \exp \left[3 \int_0^z dz' \frac{1+\tilde{w}(z')}{1+z'} \right], \quad (10)$$

From (10), a general expression for $\tilde{w}(z)$ can be obtained for any interacting dark energy model that satisfies the same conservation equation (2). As derived in Appendix C of [151], this expression is given by:

$$\tilde{w}(z) = \frac{w(z)\rho_{\text{de}}}{\rho_{\text{dm}} + \rho_{\text{de}} - \rho_{(\text{dm},0)}(1+z)^3}. \quad (11)$$

where ρ_{dm} and ρ_{de} are the dark matter and dark energy densities of the model under consideration. In the Λ CDM limit, one recovers $\tilde{w}(z) = w$.

In general, we find that when energy flows from dark energy to dark matter, a divergent phantom-crossing behaviour is observed for $\tilde{w}(z)$ [151, 272]. This divergent behaviour is not pathological, but rather an artefact of the parametrization. For illustrative purposes, the evolution of $w_{\text{dm}}^{\text{eff}}(z)$, $w_{\text{de}}^{\text{eff}}(z)$, and $\tilde{w}(z)$ for all eight models, using the mean parameter values obtained from the analysis, is shown in Fig. 7.

III. OBSERVATIONAL CONSTRAINTS

Once the set of models has been described, we aim to determine the values of the coupling parameters in each case, as well as the remaining cosmological parameters in these scenarios. We use the public Markov Chain Monte Carlo code `MontePython` [282, 283], together with modified versions of `CLASS` [284] tailored to each interacting scenario. We consider the following datasets:

- Pantheon+ Type Ia supernova data [5], calibrated with SH0ES Cepheid data.
- DESI DR2 Baryon Acoustic Oscillation data [1].
- Cosmic Clock measurements [285].
- Big Bang Nucleosynthesis as a prior on $\Omega_b h^2 = 0.02218 \pm 0.00055$ [286, 287]².

In our analyses, we consider as cosmological parameters the fractional density of dark matter Ω_{dm} , the fractional density of baryons Ω_b , the Hubble constant H_0 , and the dark energy equation of state w . In each model, we treat the interaction parameters (δ , δ_{dm} and/or δ_{de}) as free parameters, while the total matter density Ω_m is taken as a derived parameter. Due to the inclusion of Pantheon+ data, we also include the absolute magnitude of Type Ia supernovae, M , as a nuisance parameter. We assume three massive neutrinos with a total mass $\sum m_\nu = 0.06$ eV and an effective number of relativistic species $N_{\text{eff}} = 3.044$, while all other parameters are set to their default values in `CLASS`. We use flat priors with bounds summarized in Table III for each parameter. The interaction parameters are assigned unbounded flat priors, $\delta \in (-\infty, +\infty)$, except for the non-linear model given by $Q = 3H\delta \left(\frac{\rho_{\text{dm}}^2}{\rho_{\text{dm}} + \rho_{\text{de}}} \right)$, for which we impose $\delta \in [w, -0.8w/r_0]$, and the non-linear model given by $Q = 3H\delta \left(\frac{\rho_{\text{de}}^2}{\rho_{\text{dm}} + \rho_{\text{de}}} \right)$, for which we impose $\delta \in [w, -0.8wr_0]$. These bounds are required to avoid undefined dark matter or dark energy densities, in particular divisions by zero that cause $E(z)$ to diverge as the parameter space approaches the limits listed in Table I. As also shown in Table I, additional conditions can be imposed to avoid both negative energy densities and future big rip singularities. However, we do not enforce these constraints, as our goal is to investigate whether regions of parameter space associated with such features may be preferred by the data. This approach may, for example, indicate that negative energy densities are favoured in certain models.

Model / Kernel Q	Ω_{dm}	Ω_b	H_0	M	w	δ_{dm} or δ	δ_{de} or δ
ΛCDM	[0.001, 0.9]	[0.001, 0.3]	[40, 100]	[-30, -10]	—	—	—
$3H(\delta_{\text{dm}}\rho_{\text{dm}} + \delta_{\text{de}}\rho_{\text{de}})$	[0.001, 0.9]	[0.001, 0.3]	[40, 100]	[-30, -10]	[-2.00, -0.33]	$(-\infty, +\infty)$	$(-\infty, +\infty)$
$3H\delta(\rho_{\text{dm}} + \rho_{\text{de}})$	[0.001, 0.9]	[0.001, 0.3]	[40, 100]	[-30, -10]	[-2.00, -0.33]	$(-\infty, +\infty)$	—
$3H\delta(\rho_{\text{dm}} - \rho_{\text{de}})$	[0.001, 0.9]	[0.001, 0.3]	[40, 100]	[-30, -10]	[-2.00, -0.33]	$(-\infty, +\infty)$	—
$3H\delta\rho_{\text{dm}}$	[0.001, 0.9]	[0.001, 0.3]	[40, 100]	[-30, -10]	[-2.00, -0.33]	$(-\infty, +\infty)$	—
$3H\delta\rho_{\text{de}}$	[0.001, 0.9]	[0.001, 0.3]	[40, 100]	[-30, -10]	[-2.00, -0.33]	—	$(-\infty, +\infty)$
$3H\delta \left(\frac{\rho_{\text{dm}}\rho_{\text{de}}}{\rho_{\text{dm}} + \rho_{\text{de}}} \right)$	[0.001, 0.9]	[0.001, 0.3]	[40, 100]	[-30, -10]	[-2.00, -0.33]	$(-\infty, +\infty)$	—
$3H\delta \left(\frac{\rho_{\text{dm}}^2}{\rho_{\text{dm}} + \rho_{\text{de}}} \right)$	[0.001, 0.9]	[0.001, 0.3]	[40, 100]	[-30, -10]	[-2.00, -0.33]	$[w, -0.8w/r_0]$	—
$3H\delta \left(\frac{\rho_{\text{de}}^2}{\rho_{\text{dm}} + \rho_{\text{de}}} \right)$	[0.001, 0.9]	[0.001, 0.3]	[40, 100]	[-30, -10]	[-2.00, -0.33]	—	$[w, -0.8w r_0]$

TABLE III. **Flat priors used for all cosmological and coupling parameters** for ΛCDM and the interacting dark energy models. The coupling parameters δ , δ_{dm} , and δ_{de} are assigned unbounded flat priors, except for the last two non-linear models, where bounds are imposed to avoid undefined densities, as summarized in Table I. Here,

$$r_0 = \Omega_{\text{dm},0}/(1 - \Omega_{\text{m},0}).$$

III.1. Linear models

We begin by considering the most general linear model in which both interaction parameters, δ_{dm} and δ_{de} , are allowed to vary ($Q = 3H(\delta_{\text{dm}}\rho_{\text{dm}} + \delta_{\text{de}}\rho_{\text{de}})$), as well as the cases in which only one of them is allowed to vary ($Q = 3H\delta\rho_{\text{dm}}$ and $Q = 3H\delta\rho_{\text{de}}$). These models were introduced in Section II.1. In Table IV, we present the results obtained using Pantheon+ and DESI DR2 data, while Table V shows the corresponding results when additional information from

² The same prior is used in the DESI DR2 analysis [1] to break the well-known degeneracy in $H_0 r_d$.

Cosmic Clocks and BBN is also incorporated. For a clearer visualization, the contour plots corresponding to the latter case are shown in Fig. 1.

Takeaways from MCMC analysis for $Q = 3H(\delta_{\text{dm}}\rho_{\text{dm}} + \delta_{\text{de}}\rho_{\text{de}})$, $Q = 3H\delta\rho_{\text{dm}}$, and $Q = 3H\delta\rho_{\text{de}}$:

- A detection of the interaction sourced by δ_{dm} is found, while the constraining power for the interaction parameter δ_{de} remains very poor. This lack of sensitivity to δ_{de} , despite obtaining consistent results for δ_{dm} , persists even when both interactions are allowed to act simultaneously. This indicates that the data do not provide sufficient constraining power to isolate the effects of δ_{de} , since at the background level an interaction proportional to ρ_{de} largely mimics a dynamical dark energy expansion history and is therefore highly degenerate with non-interacting DDE models when using background observables alone, whereas an interaction proportional to ρ_{dm} directly modifies the matter dilution rate and can be more effectively constrained.
- Since $\delta_{\text{dm}} < 0$, the models predict energy flow from dark matter to dark energy and the presence of negative dark energy at some point in the past. Since δ_{de} is not well constrained, negative values are still allowed, which could in turn predict negative dark matter densities in the future.
- The matter content is strongly affected by the nature of the interaction. When both interactions are simultaneously active, or when only δ_{de} is allowed to vary, a large increase in the total matter density is observed. Conversely, when only δ_{dm} is allowed to vary, a mild decrease in the matter density is found.
- In addition, phantom-like dark energy behaviour appears whenever the interaction parameter δ_{de} is included, either alone or in combination with δ_{dm} . This points toward an effective equation of state $w < -1$, although such an effect must be interpreted cautiously, since it may simply arise from parameter degeneracies involving w and δ_{de} . For the interaction $Q = 3H\delta\rho_{\text{de}}$, dark energy has an effective equation of state $w_{\text{de}}^{\text{eff}} = w + \delta$, as obtained from (9). This implies that, even if $w < -1$, one may still have $w_{\text{de}}^{\text{eff}} > -1$, thereby avoiding consequences such as a future big rip singularity. This behaviour is illustrated by the regions of parameter space inside and outside the green mesh in panel 5 of Fig. 6. See [150] for a detailed analysis of the consequences of $w < -1$ and big rip singularities for the linear IDE models considered here.

We now consider the remaining linear models in which the interaction parameters satisfy the conditions $\delta_{\text{dm}} = \delta_{\text{de}} \equiv \delta$ ($Q = 3H\delta(\rho_{\text{dm}} + \rho_{\text{de}})$) or $\delta_{\text{dm}} = -\delta_{\text{de}} \equiv \delta$ ($Q = 3H\delta(\rho_{\text{dm}} - \rho_{\text{de}})$), introduced in Section II.1. We display in Table IV the results obtained using Pantheon+ and DESI DR2 data, and in Table V those obtained when additional information from Cosmic Clocks and BBN datasets is incorporated. For a clearer visualization of the behaviour of these models, we also show the contour plots for the latter case in Fig. 2.

Takeaways from MCMC analysis for $Q = 3H\delta(\rho_{\text{dm}} + \rho_{\text{de}})$ and $Q = 3H\delta(\rho_{\text{dm}} - \rho_{\text{de}})$:

- A detection of the interaction parameter δ is obtained in both cases, pointing toward a non-negligible exchange of energy between the dark sectors. Since $\delta < 0$ in both cases, there is a clear preference for an initial energy flow from dark matter to dark energy, with the interaction $Q = 3H\delta(\rho_{\text{dm}} - \rho_{\text{de}})$ later switching to an energy flow from dark energy to dark matter. As discussed in [150] and shown in Table II, this implies the presence of negative dark energy in the past for both models, and additionally predicts negative dark matter in the future for the interaction $Q = 3H\delta(\rho_{\text{dm}} + \rho_{\text{de}})$.
- Regarding the matter content, we observe a mild decrease in the total matter density compared to Λ CDM, although this effect is slightly smaller for the interaction $Q = 3H\delta(\rho_{\text{dm}} - \rho_{\text{de}})$.

III.2. Non-linear models

Considering now the non-linear models presented in Section II.2, we display in Table IV the results obtained using Pantheon+ and DESI DR2 data, and in Table V those obtained when including the additional information from Pantheon+, DESI DR2, Cosmic Clocks, and BBN data. For a clearer visualization of these results, we also show the corresponding contour plots for the latter case in Figure 3.

Takeaways from MCMC analysis for $Q = 3H\delta\left(\frac{\rho_{\text{dm}}\rho_{\text{de}}}{\rho_{\text{dm}} + \rho_{\text{de}}}\right)$, $Q = 3H\delta\left(\frac{\rho_{\text{dm}}^2}{\rho_{\text{dm}} + \rho_{\text{de}}}\right)$ and $Q = 3H\delta\left(\frac{\rho_{\text{de}}^2}{\rho_{\text{dm}} + \rho_{\text{de}}}\right)$:

- We find a mild detection of the three non-linear interactions from both combinations of datasets. For $Q = 3H\delta\left(\frac{\rho_{\text{dm}}\rho_{\text{de}}}{\rho_{\text{dm}} + \rho_{\text{de}}}\right)$ and $Q = 3H\delta\left(\frac{\rho_{\text{dm}}^2}{\rho_{\text{dm}} + \rho_{\text{de}}}\right)$, there is a preference for energy flow from dark matter to dark energy ($\delta < 0$), while for $Q = 3H\delta\left(\frac{\rho_{\text{de}}^2}{\rho_{\text{dm}} + \rho_{\text{de}}}\right)$ there is a preference for energy flow from dark energy to dark matter

Model / Kernel Q	Ω_{dm}	H_0	M	w	δ_{dm} or δ	δ_{de} or δ
ΛCDM	$0.2648^{+0.0080(0.016)}_{-0.0080(0.015)}$	$71.15^{+0.70(1.4)}_{-0.70(1.4)}$	$-19.323^{+0.022(0.042)}_{-0.022(0.042)}$	—	—	—
$3H(\delta_{\text{dm}}\rho_{\text{dm}} + \delta_{\text{de}}\rho_{\text{de}})$	$0.32^{+0.18(0.30)}_{-0.18(0.30)}$	$73.64^{+0.99(2.0)}_{-0.99(1.9)}$	$-19.241^{+0.028(0.056)}_{-0.028(0.055)}$	$-1.10^{+0.45(0.70)}_{-0.32(0.79)}$	$-0.0068^{+0.0032(0.0054)}_{-0.0026(0.0060)}$	$0.20^{+0.32(0.79)}_{-0.46(0.71)}$
$3H\delta(\rho_{\text{dm}} + \rho_{\text{de}})$	$0.238^{+0.011(0.021)}_{-0.011(0.022)}$	$73.63^{+0.98(1.9)}_{-0.98(1.9)}$	$-19.242^{+0.028(0.055)}_{-0.028(0.055)}$	$-0.896^{+0.045(0.087)}_{-0.045(0.089)}$	$-0.0077^{+0.0023(0.0042)}_{-0.0021(0.0046)}$	—
$3H\delta(\rho_{\text{dm}} - \rho_{\text{de}})$	$0.2501^{+0.0083(0.017)}_{-0.0083(0.016)}$	$73.63^{+0.99(2.0)}_{-0.99(1.9)}$	$-19.242^{+0.028(0.055)}_{-0.028(0.055)}$	$-0.911^{+0.041(0.079)}_{-0.041(0.081)}$	$-0.0076^{+0.0022(0.0041)}_{-0.0020(0.0044)}$	—
$3H\delta\rho_{\text{dm}}$	$0.2441^{+0.0095(0.019)}_{-0.0095(0.019)}$	$73.63^{+0.97(1.9)}_{-0.97(1.9)}$	$-19.242^{+0.028(0.055)}_{-0.028(0.055)}$	$-0.903^{+0.043(0.083)}_{-0.043(0.085)}$	$-0.0077^{+0.0022(0.0042)}_{-0.0022(0.0045)}$	—
$3H\delta\rho_{\text{de}}$	$0.351^{+0.20(0.33)}_{-0.17(0.35)}$	$72.90^{+0.97(1.9)}_{-0.97(1.9)}$	$-19.282^{+0.026(0.052)}_{-0.026(0.052)}$	$-1.30^{+0.42(0.71)}_{-0.37(0.70)}$	—	$0.25^{+0.37(0.75)}_{-0.42(0.72)}$
$3H\delta\left(\frac{\rho_{\text{dm}}\rho_{\text{de}}}{\rho_{\text{dm}}+\rho_{\text{de}}}\right)$	$0.074^{+0.041(0.11)}_{-0.057(0.073)}$	$72.93^{+0.96(1.9)}_{-0.96(1.9)}$	$-19.262^{+0.027(0.053)}_{-0.027(0.053)}$	$-0.711^{+0.10(0.18)}_{-0.077(0.20)}$	$-0.85^{+0.38(0.73)}_{-0.34(0.76)}$	—
$3H\delta\left(\frac{\rho_{\text{dm}}^2}{\rho_{\text{dm}}+\rho_{\text{de}}}\right)$	$0.2467^{+0.0091(0.018)}_{-0.0091(0.018)}$	$73.63^{+0.98(2.0)}_{-0.98(1.9)}$	$-19.242^{+0.028(0.055)}_{-0.028(0.055)}$	$-0.908^{+0.042(0.082)}_{-0.042(0.083)}$	$-0.0076^{+0.0023(0.0041)}_{-0.0020(0.0044)}$	—
$3H\delta\left(\frac{\rho_{\text{de}}^2}{\rho_{\text{dm}}+\rho_{\text{de}}}\right)$	$0.428^{+0.059(0.070)}_{-0.017(0.11)}$	$72.94^{+0.96(1.9)}_{-0.96(1.9)}$	$-19.270^{+0.027(0.052)}_{-0.027(0.052)}$	$-1.277^{+0.045(0.17)}_{-0.10(0.13)}$	—	$0.76^{+0.38(0.44)}_{-0.15(0.59)}$

TABLE IV. **Pantheon+ & DESI DR2** – mean values and 68% constraints (with 95% limits in parentheses) for ΛCDM and interacting dark energy models. **Note:** $\Omega_{\text{m}} = \Omega_{\text{dm}} + \Omega_b$, with $\Omega_b = 0.048$ fixed for all models.

Model / Kernel Q	Ω_{dm}	Ω_b	H_0	M	w	δ_{dm} or δ	δ_{de} or δ
ΛCDM	$0.2596^{+0.0079(0.016)}_{-0.0079(0.015)}$	$0.04713^{+0.00076(0.0015)}_{-0.00076(0.0015)}$	$70.04^{+0.49(0.96)}_{-0.49(0.95)}$	$-19.358^{+0.015(0.030)}_{-0.015(0.030)}$	—	—	—
$3H(\delta_{\text{dm}}\rho_{\text{dm}} + \delta_{\text{de}}\rho_{\text{de}})$	$0.32^{+0.18(0.29)}_{-0.18(0.30)}$	$0.0426^{+0.0015(0.029)}_{-0.0015(0.029)}$	$72.21^{+0.85(1.7)}_{-0.85(1.7)}$	$-19.287^{+0.024(0.047)}_{-0.024(0.047)}$	$-1.13^{+0.46(0.72)}_{-0.33(0.80)}$	$-0.0075^{+0.0034(0.0058)}_{-0.0028(0.0064)}$	$0.21^{+0.33(0.80)}_{-0.47(0.72)}$
$3H\delta(\rho_{\text{dm}} + \rho_{\text{de}})$	$0.239^{+0.010(0.020)}_{-0.010(0.021)}$	$0.0426^{+0.0015(0.028)}_{-0.0015(0.028)}$	$72.21^{+0.85(1.7)}_{-0.85(1.7)}$	$-19.287^{+0.024(0.047)}_{-0.024(0.047)}$	$-0.916^{+0.043(0.084)}_{-0.043(0.086)}$	$-0.0086^{+0.0023(0.0046)}_{-0.0023(0.0046)}$	—
$3H\delta(\rho_{\text{dm}} - \rho_{\text{de}})$	$0.2525^{+0.0080(0.015)}_{-0.0080(0.015)}$	$0.0426^{+0.0014(0.028)}_{-0.0014(0.028)}$	$72.22^{+0.84(1.7)}_{-0.84(1.6)}$	$-19.287^{+0.024(0.046)}_{-0.024(0.046)}$	$-0.934^{+0.040(0.077)}_{-0.040(0.080)}$	$-0.0083^{+0.0022(0.0042)}_{-0.0022(0.0042)}$	—
$3H\delta\rho_{\text{dm}}$	$0.2459^{+0.0091(0.018)}_{-0.0091(0.018)}$	$0.0426^{+0.0015(0.028)}_{-0.0015(0.028)}$	$72.21^{+0.85(1.7)}_{-0.85(1.6)}$	$-19.287^{+0.024(0.047)}_{-0.024(0.047)}$	$-0.925^{+0.041(0.080)}_{-0.041(0.082)}$	$-0.0085^{+0.0022(0.0043)}_{-0.0022(0.0045)}$	—
$3H\delta\rho_{\text{de}}$	$0.36^{+0.20(0.33)}_{-0.16(0.35)}$	$0.0456^{+0.0013(0.025)}_{-0.0013(0.025)}$	$70.89^{+0.85(1.7)}_{-0.76(1.5)}$	$-19.339^{+0.020(0.038)}_{-0.020(0.039)}$	$-1.32^{+0.41(0.71)}_{-0.37(0.68)}$	—	$0.27^{+0.37(0.75)}_{-0.42(0.72)}$
$3H\delta\left(\frac{\rho_{\text{dm}}\rho_{\text{de}}}{\rho_{\text{dm}}+\rho_{\text{de}}}\right)$	$0.083^{+0.044(0.12)}_{-0.061(0.082)}$	$0.0449^{+0.0012(0.025)}_{-0.0012(0.024)}$	$71.06^{+0.74(1.5)}_{-0.74(1.4)}$	$-19.319^{+0.021(0.041)}_{-0.021(0.041)}$	$-0.731^{+0.11(0.19)}_{-0.080(0.21)}$	$-0.78^{+0.33(0.63)}_{-0.33(0.65)}$	—
$3H\delta\left(\frac{\rho_{\text{dm}}^2}{\rho_{\text{dm}}+\rho_{\text{de}}}\right)$	$0.2488^{+0.0087(0.017)}_{-0.0087(0.017)}$	$0.0426^{+0.0015(0.029)}_{-0.0015(0.028)}$	$72.22^{+0.85(1.7)}_{-0.85(1.6)}$	$-19.287^{+0.024(0.047)}_{-0.024(0.047)}$	$-0.930^{+0.041(0.079)}_{-0.041(0.081)}$	$-0.0084^{+0.0022(0.0043)}_{-0.0022(0.0044)}$	—
$3H\delta\left(\frac{\rho_{\text{de}}^2}{\rho_{\text{dm}}+\rho_{\text{de}}}\right)$	$0.426^{+0.062(0.073)}_{-0.018(0.11)}$	$0.0451^{+0.0013(0.025)}_{-0.0013(0.024)}$	$71.02^{+0.74(1.5)}_{-0.74(1.5)}$	$-19.327^{+0.020(0.039)}_{-0.020(0.039)}$	$-1.273^{+0.060(0.19)}_{-0.11(0.16)}$	—	$0.74^{+0.38(0.46)}_{-0.17(0.49)}$

TABLE V. **Pantheon+, DESI DR2, Cosmic Clocks & BBN** – mean values and 68% constraints (with 95% limits in parentheses) for the cosmological and nuisance parameters in ΛCDM and the eight interacting dark energy models.

$(\delta > 0)$. In the case of $Q = 3H\delta\left(\frac{\rho_{\text{dm}}\rho_{\text{de}}}{\rho_{\text{dm}}+\rho_{\text{de}}}\right)$, since $\delta < 0$, we obtain a negative dark energy density in the past, while for the other two cases the dark sector densities remain positive at all times. For $Q = 3H\delta\left(\frac{\rho_{\text{de}}^2}{\rho_{\text{dm}}+\rho_{\text{de}}}\right)$, the interaction parameter δ appears to approach the upper limit for which the energy densities remain defined and positive, $\delta = -wr_0$, as seen in the last panel of Figure 6. The parameters cannot cross this boundary due to the artificial prior limits imposed to avoid these unphysical scenarios, as summarized in Table III.

- In $Q = 3H\delta\left(\frac{\rho_{\text{dm}}\rho_{\text{de}}}{\rho_{\text{dm}}+\rho_{\text{de}}}\right)$, there is a large decrease in the total matter content, primarily driven by a significant reduction in the interacting dark matter component. Nevertheless, the constraints on the dark matter and total matter density parameters remain weak, since a strong degeneracy persists between Ω_{dm} and the interaction parameter δ , as seen in Fig. 3. Conversely, in $Q = 3H\delta\left(\frac{\rho_{\text{de}}^2}{\rho_{\text{dm}}+\rho_{\text{de}}}\right)$, we observe the opposite trend: a significant increase in the matter density, carried almost entirely by a substantial rise in the interacting dark matter component. Once again, the robustness of these results is limited by the strong degeneracy between Ω_{dm} and δ .
- In addition, phantom-like dark energy behaviour ($w < -1$) appears in the case of $Q = 3H\delta\left(\frac{\rho_{\text{de}}^2}{\rho_{\text{dm}}+\rho_{\text{de}}}\right)$, similar to what is found for the linear models when δ_{de} is included. This possibility must be interpreted with care, since it may be a consequence of the strong degeneracy between the dark energy equation of state w and the interaction parameter δ (see Fig. 3). Even when $w < -1$, the effective dark energy equation of state $w_{\text{de}}^{\text{eff}}$ given by (9) may not lie in the phantom regime. As a result, the best-fit value can be located in a region where $w_{\text{de}}^{\text{eff}} > -1$, and associated phantom features such as a future big rip singularity may be avoided, as illustrated in the last panel of Figure 6.

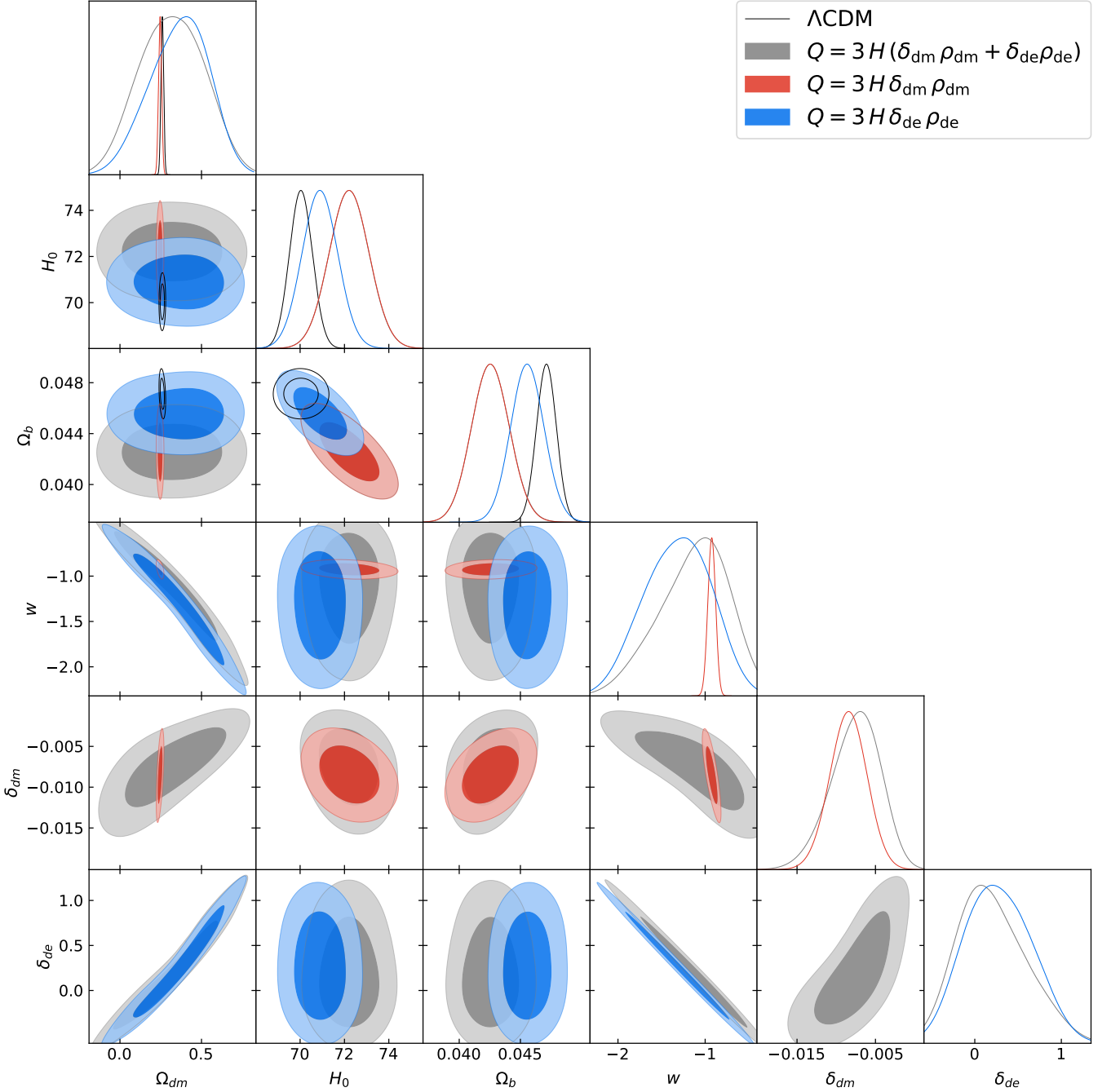


FIG. 1. **Pantheon+, DESI DR2, Cosmic Clocks & BBN** – One-dimensional posterior distributions and two-dimensional contours obtained for several parameters for the reference Λ CDM model and the models given by $Q = 3H\delta\rho_{\text{dm}}$ and $Q = 3H\delta\rho_{\text{de}}$, discussed in Section II.1.

III.3. Statistical analysis: $\Delta\chi^2$ & ΔAIC

In order to assess the large number of models presented in this work, we compare them statistically to the reference scenario, the Λ CDM model. Our first comparison relies on the relative χ^2 value with respect to Λ CDM, defined as $\Delta\chi^2 = \chi^2_{\text{model}} - \chi^2_{\Lambda\text{CDM}}$, such that negative values correspond to a better fit to the data. The relative values are displayed in Table VI.

Regarding the linear models, we find that they provide a substantial improvement in the fit, with the only exception being $Q = 3H\delta\rho_{\text{de}}$, for which the preference is smaller, although still present. These results hold for both dataset

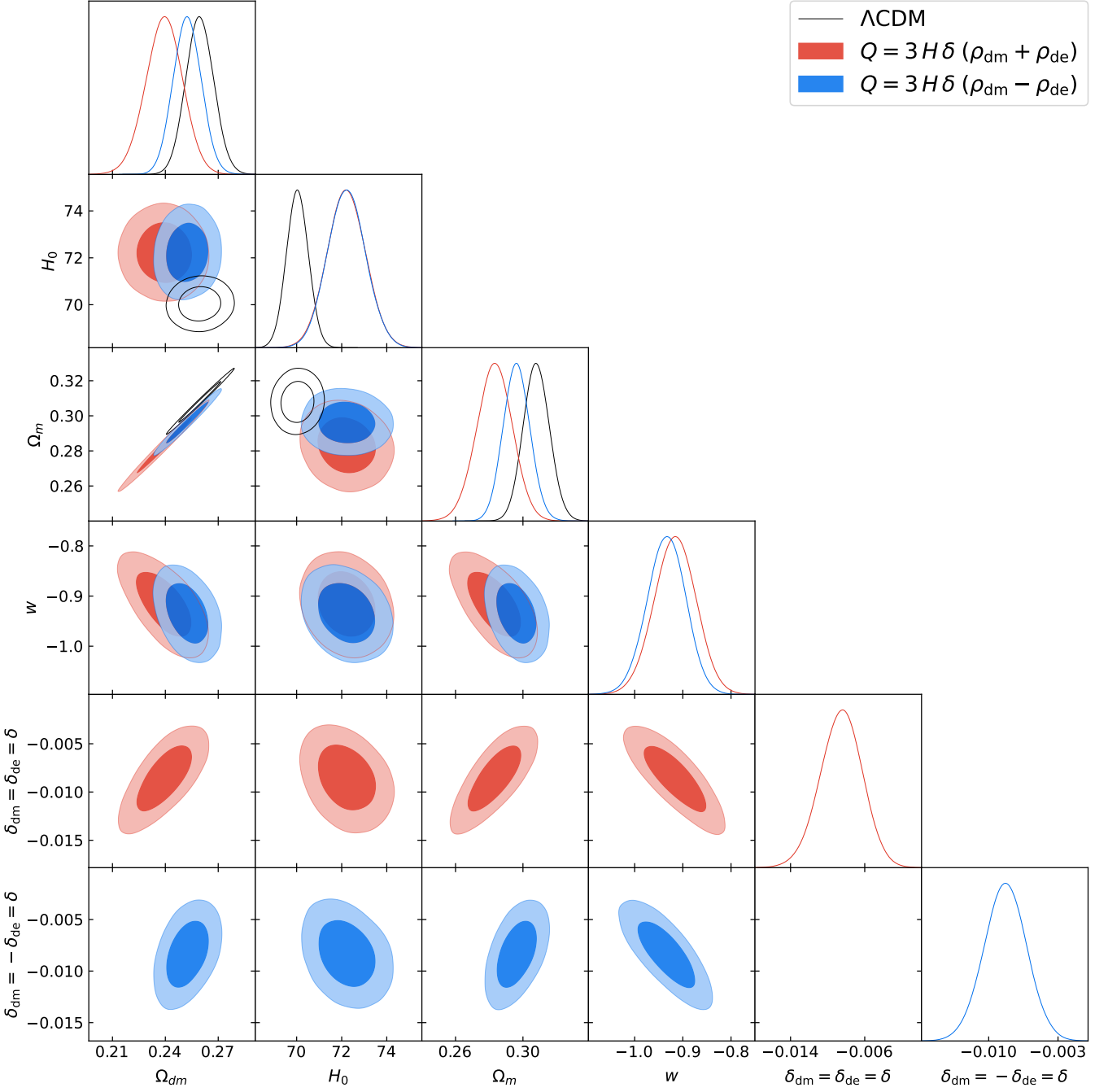


FIG. 2. **Pantheon+, DESI DR2, Cosmic Clocks & BBN** – One-dimensional posterior distributions and two-dimensional contours obtained for several parameters for the reference Λ CDM model and the models given by $Q = 3H\delta(\rho_{\text{dm}} + \rho_{\text{de}})$ and $Q = 3H\delta(\rho_{\text{dm}} - \rho_{\text{de}})$, discussed in Section II.1.

combinations considered, namely Pantheon+ and DESI DR2, and Pantheon+, DESI DR2, Cosmic Clocks, and BBN. However, when Cosmic Clocks and BBN data are added, the statistical preferences are reduced, although they remain clear for all linear models, with the previously mentioned exception of $Q = 3H\delta\rho_{\text{de}}$. In this specific case, the inclusion of these datasets causes the statistical preference to almost vanish.

For the non-linear models, we also observe a remarkable improvement in the fitting performance according to the χ^2 criterion, particularly for $Q = 3H\delta\left(\frac{\rho_{\text{dm}}^2}{\rho_{\text{dm}} + \rho_{\text{de}}}\right)$, which behaves similarly to $Q = 3H\delta\rho_{\text{dm}}$. Conversely, $Q = 3H\delta\left(\frac{\rho_{\text{de}}^2}{\rho_{\text{dm}} + \rho_{\text{de}}}\right)$, which behaves similarly to $Q = 3H\delta\rho_{\text{de}}$, performs worst among the non-linear models. Once again,

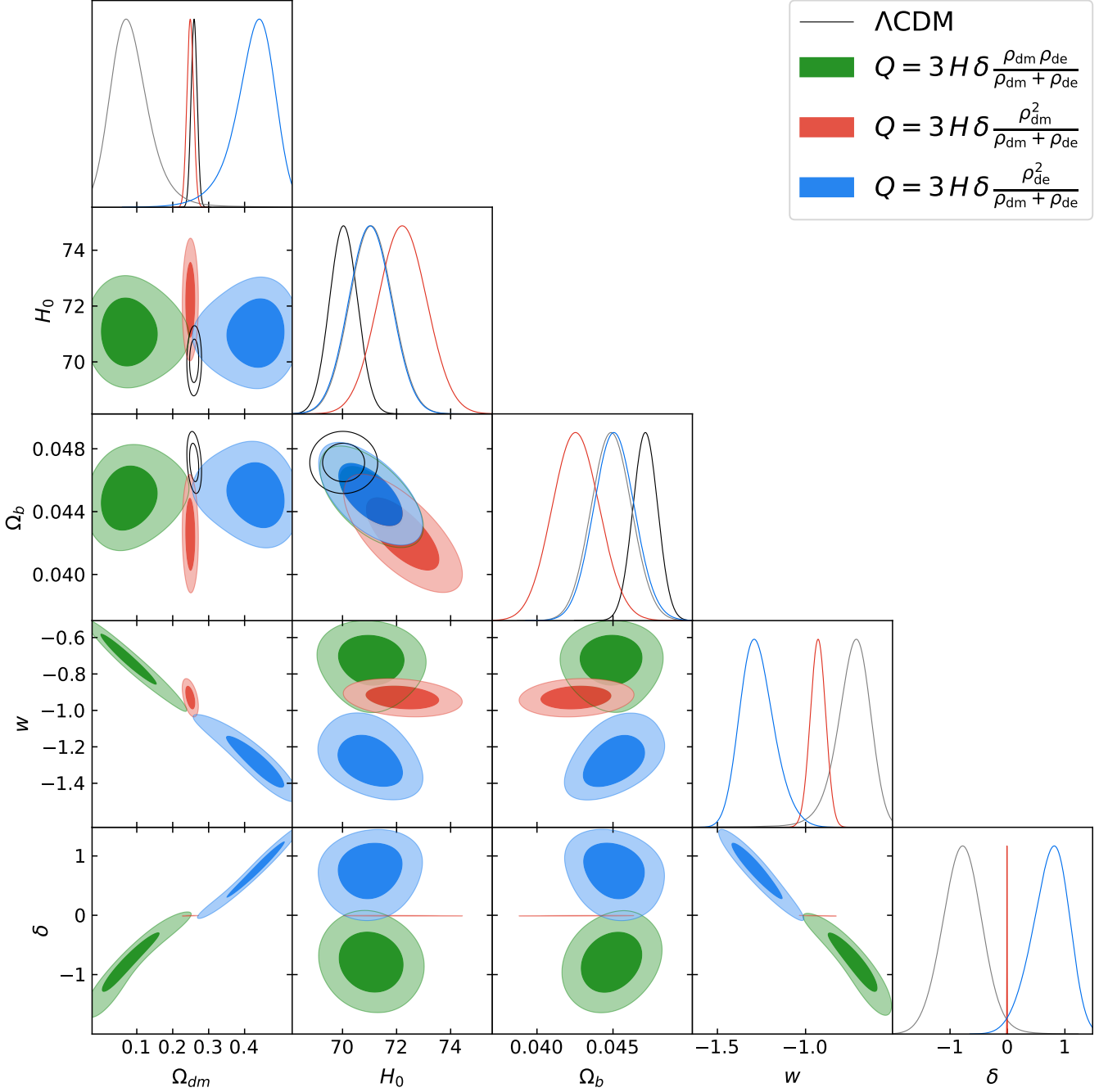


FIG. 3. **Pantheon+, DESI DR2, Cosmic Clocks & BBN** – One-dimensional posterior distributions and two-dimensional contours obtained for several parameters for the reference Λ CDM model and the models given by $Q = 3H\delta \left(\frac{\rho_{\text{dm}}\rho_{\text{de}}}{\rho_{\text{dm}} + \rho_{\text{de}}} \right)$, $Q = 3H\delta \left(\frac{\rho_{\text{dm}}^2}{\rho_{\text{dm}} + \rho_{\text{de}}} \right)$, and $Q = 3H\delta \left(\frac{\rho_{\text{de}}^2}{\rho_{\text{dm}} + \rho_{\text{de}}} \right)$, discussed in Section II.2.

the inclusion of Cosmic Clocks and BBN data reduces the level of statistical preference.

However, we must take into account that we are comparing models with different numbers of parameters. In the interacting scenarios, the dark energy equation-of-state parameter is allowed to vary freely, and in addition we introduce the interaction parameter δ in each model, or the pair of interaction parameters δ_{dm} and δ_{de} in the case of $Q = 3H(\delta_{\text{dm}}\rho_{\text{dm}} + \delta_{\text{de}}\rho_{\text{de}})$. Consequently, these models involve two or even three additional parameters with respect to Λ CDM. It is well known that increasing the number of parameters generally leads to a better fit, but this does not necessarily imply a genuine improvement. Therefore, it is necessary to assess the statistical preference for these

Model / Kernel Q	Pantheon+ & DESI DR2		Pantheon+, DESI DR2, CC & BBN	
	$\Delta\chi^2$	ΔAIC	$\Delta\chi^2$	ΔAIC
ΛCDM	—	—	—	—
$3H(\delta_{\text{dm}}\rho_{\text{dm}} + \delta_{\text{de}}\rho_{\text{de}})$	-21.96	-15.96	-17.76	-11.76
$3H\delta(\rho_{\text{dm}} + \rho_{\text{de}})$	-21.94	-17.94	-17.76	-13.76
$3H\delta(\rho_{\text{dm}} - \rho_{\text{de}})$	-21.96	-17.96	-17.74	-13.74
$3H\delta\rho_{\text{dm}}$	-21.94	-17.94	-17.74	-13.74
$3H\delta\rho_{\text{de}}$	-7.52	-3.52	-2.34	+1.66
$3H\delta\left(\frac{\rho_{\text{dm}}\rho_{\text{de}}}{\rho_{\text{dm}} + \rho_{\text{de}}}\right)$	-16.14	-12.14	-10.28	-6.28
$3H\delta\left(\frac{\rho_{\text{dm}}^2}{\rho_{\text{dm}} + \rho_{\text{de}}}\right)$	-21.94	-17.94	-17.76	-13.76
$3H\delta\left(\frac{\rho_{\text{de}}^2}{\rho_{\text{dm}} + \rho_{\text{de}}}\right)$	-15.02	-11.02	-9.46	-5.46

TABLE VI. Differences in χ^2 and in the Akaike Information Criterion (AIC) relative to ΛCDM for all interacting dark energy models considered. The interacting models include $\Delta k = 2$ additional parameters (w, δ), except for $Q = 3H(\delta_{\text{dm}}\rho_{\text{dm}} + \delta_{\text{de}}\rho_{\text{de}})$, which has $\Delta k = 3$. Negative ΔAIC values indicate improved performance relative to ΛCDM .

models by accounting for the penalty associated with the additional degrees of freedom. To this end, we rely on the Akaike Information Criterion, defined as $\text{AIC} = \chi^2 + 2 \text{d.o.f.}$ [288]. We define the relative difference, as before, as $\Delta\text{AIC} = \text{AIC}_{\text{model}} - \text{AIC}_{\Lambda\text{CDM}}$ to assess the goodness of fit.

Regarding the values of ΔAIC displayed in Table VI, we find that the linear models, with the exception of $Q = 3H\delta\rho_{\text{de}}$, are strongly preferred compared to the reference ΛCDM model, regardless of the dataset considered. This result, combined with the non-zero values of the coupling parameters in each model, suggests that further investigation of these scenarios is warranted. However, it should be noted that the values obtained for the coupling parameters are extraordinarily small and, as a consequence, the resulting deviations from the reference scenario are very limited. In the specific case of $Q = 3H\delta\rho_{\text{de}}$, the statistical preference is very modest when using Pantheon+ and DESI DR2 data, and it essentially vanishes once Cosmic Clocks and BBN data are included.

For the non-linear models, we also find a strong preference in all three cases when using Pantheon+ and DESI DR2 data, while this preference becomes more modest once Cosmic Clocks and BBN data are added. In this respect, the situation differs from that of the linear models. The values of the coupling parameters obtained from the constraints in each case are relatively large, implying that the associated effects may be significant and allowing these models to be distinguished from ΛCDM . In addition, we note that for $Q = 3H\delta\left(\frac{\rho_{\text{de}}^2}{\rho_{\text{dm}} + \rho_{\text{de}}}\right)$ the coupling parameter δ lies close to the upper bound imposed by our priors in Table III to avoid undefined densities, which renders this constraint somewhat artificial compared to those obtained for the other models.

III.4. Cosmological implications and comparison between models

When comparing the eight interaction models, several interesting trends emerge, which we summarize according to the following properties (with figures and tables illustrating or clarifying these statements indicated in brackets):

- **Direction of energy transfer** (Figures 4 and 5, and Table VII): For the most general linear interaction, $Q = 3H(\delta_{\text{dm}}\rho_{\text{dm}} + \delta_{\text{de}}\rho_{\text{de}})$, as well as for $Q = 3H\delta(\rho_{\text{dm}} - \rho_{\text{de}})$, a preference is found for a sign-switching interaction, with energy flowing from dark matter to dark energy at early times (corresponding to $\delta_{\text{dm}} < 0$) and from dark energy to dark matter at later times (corresponding to $\delta_{\text{de}} > 0$). This behaviour is in agreement with recent reconstructions of the interaction kernel Q from data, where sign-switching behaviour has been suggested in [207, 217]. For all other interactions, sign-switching behaviour is not possible. Instead, for the remaining models we observe a preference for energy flow from dark matter to dark energy when $Q \propto \rho_{\text{dm}}$ in any form. The only exceptions, where energy flows from dark energy to dark matter, occur for interactions proportional to ρ_{de} , specifically $Q = 3H\delta\rho_{\text{de}}$ and $Q = 3H\delta\left(\frac{\rho_{\text{de}}^2}{\rho_{\text{dm}} + \rho_{\text{de}}}\right)$, which, as noted in Section III.3, exhibit the weakest statistical preference among the interactions considered.
- **Presence of negative energies** (Figure 6 and Table VII): As discussed above, most models prefer energy flow from dark matter to dark energy, which in turn leads to negative dark energy densities in the past [150], as illustrated in Figure 6. Other observational indications hinting at $\rho_{\text{de}} < 0$ in the past can also be found

in [137, 261, 267]. Conversely, interactions for which $Q \propto \rho_{\text{de}}$ exhibit energy flow from dark energy to dark matter and therefore avoid negative energy densities, while the interaction $Q = 3H\delta \left(\frac{\rho_{\text{dm}}\rho_{\text{de}}}{\rho_{\text{dm}}+\rho_{\text{de}}} \right)$ always yields positive energy densities across the entire parameter space.

- **Future big rip singularities** (Figure 6): Future big rip singularities can also occur, and are most likely for the interaction $Q = 3H\delta\rho_{\text{de}}$ (see the overlap between the green mesh and the contour plots in Figure 6), although the parameter space is not sufficiently well constrained to draw definitive conclusions. For the same interaction, it is worth noting that the 65% and 95% confidence intervals may cross the upper positive-energy limit for δ , which could lead to a past non-singular bounce, a feature of interacting models that will be discussed in detail in future work. We again emphasise that the predicted negative energies and future singularities do not necessarily represent pathologies of the theory, as they may instead indicate that the model has been pushed beyond its domain of applicability.
- **Possible early-time instabilities** (Figure 6 and Table VIII): As discussed in Section II.3, the early-time stability of the models may be assessed *a priori* from the sign of the doom factor \mathbf{d} in (8), where $\mathbf{d} < 0$ implies a stable model. Using the mean values obtained in the previous section, this analysis leads to the results summarized in Table VIII, where half of the models are found to be free from instabilities. We emphasize once more that this analysis is preliminary, and that a full perturbation study for each model will be carried out in future work.
- **Phantom crossing of $w_{\text{de}}^{\text{eff}}(z)$** (Figure 7): A clear trend is observed in the evolution of $w_{\text{de}}^{\text{eff}}(z)$ in the top panel of Figure 7, which indicates when ρ_{de} increases or decreases over time. For seven of the eight models, we observe phantom-crossing behaviour, with the dark energy density decreasing at low redshift ($w_{\text{de}}^{\text{eff}} > -1$) and increasing at higher redshift ($w_{\text{de}}^{\text{eff}} < -1$). The only exception is $Q = 3H\delta\rho_{\text{de}}$, for which $w_{\text{de}}^{\text{eff}} = w + \delta$ is constant [150]. This increase and subsequent decrease of dark energy density was also suggested by the DESI collaboration [52], and may be explained by interactions between the dark sectors, as noted in [207]. Care is required when comparing these results, since our models also involve dark matter with non-cold behaviour, $w_{\text{dm}}^{\text{eff}} \neq 0$, as illustrated in the middle panel of Figure 7. Finally, as discussed in Section II.4, interaction models with energy flow from dark energy to dark matter also exhibit a divergent phantom crossing for the reconstructed dark energy equation of state $\tilde{w}(z)$ from (11). As shown in the bottom panel of Figure 7, these models have $\tilde{w}(z) < -1$ at low redshift and $\tilde{w}(z) > -1$ at higher redshift. In contrast, interactions for which energy flows from dark matter to dark energy do not exhibit any phantom-crossing behaviour.

Interaction Q	Preferred energy flow	$\rho_{\text{dm},\text{past}}$	$\rho_{\text{dm},\text{future}}$	$\rho_{\text{de},\text{past}}$	$\rho_{\text{de},\text{future}}$
$3H(\delta_{\text{dm}}\rho_{\text{dm}} + \delta_{\text{de}}\rho_{\text{de}})$	DM \rightarrow DE followed by DE \rightarrow DM	+	+	-	+
$3H\delta(\rho_{\text{dm}} + \rho_{\text{de}})$	DM \rightarrow DE	+	-	-	+
$3H\delta(\rho_{\text{dm}} - \rho_{\text{de}})$	DM \rightarrow DE followed by DE \rightarrow DM	+	+	-	+
$3H\delta\rho_{\text{dm}}$	DM \rightarrow DE	+	+	-	+
$3H\delta\rho_{\text{de}}$	DE \rightarrow DM	+	+	+	+
$3H\delta \left(\frac{\rho_{\text{dm}}\rho_{\text{de}}}{\rho_{\text{dm}}+\rho_{\text{de}}} \right)$	DM \rightarrow DE	+	+	+	+
$3H\delta \left(\frac{\rho_{\text{dm}}^2}{\rho_{\text{dm}}+\rho_{\text{de}}} \right)$	DM \rightarrow DE	+	+	-	+
$3H\delta \left(\frac{\rho_{\text{de}}^2}{\rho_{\text{dm}}+\rho_{\text{de}}} \right)$	DE \rightarrow DM	+	+	+	+

TABLE VII. Summary of the inferred direction of energy flow and the positivity of dark matter and dark energy for each model, based on the posteriors reported in Tables IV and V. It should be noted that, since not all parameters are well constrained, alternative scenarios are still allowed. The direction of energy flow is visualized for linear models in Figure 4 and for non-linear models in Figure 5. See Table II and Figure 6 for a more detailed understanding of the parameter space and its consequences for each model.

IV. CONCLUSIONS

In this study, we constrained interacting dark energy models using two different combinations of late-time datasets. The first combination included only Pantheon+ Type Ia supernovae and DESI DR2 baryon acoustic oscillation data, while the second combination additionally incorporated Cosmic Clocks and Big Bang Nucleosynthesis. The models

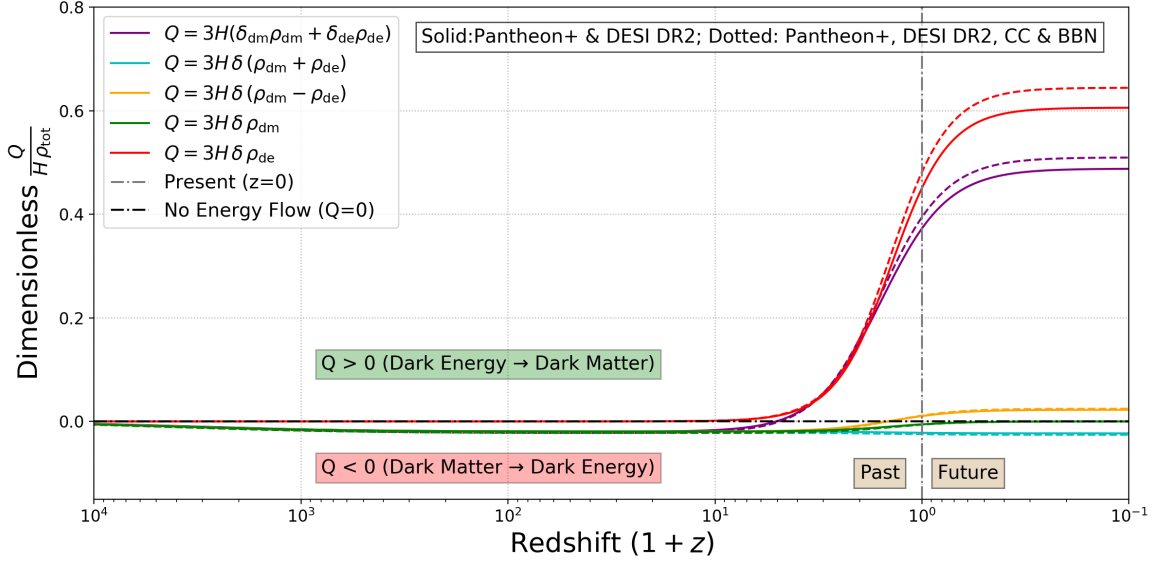


FIG. 4. Direction of energy transfer vs redshift for linear interactions, using the mean values obtained in Tables IV and V. The direction of energy transfer is also summarised in Table VII. Here we see that the most general form, $Q = 3H(\delta_{dm}\rho_{dm} + \delta_{de}\rho_{de})$, exhibits sign-switching behaviour. It behaves similarly to $Q = 3H\delta\rho_{dm}$ in the distant past, with a small relative energy flow from dark matter to dark energy, but behaves closer to $Q = 3H\delta\rho_{de}$ in the more recent past and the predicted future, where a larger relative energy flow from dark energy to dark matter is observed. This sign-changing behaviour, with similar initial and final directions of energy transfer, is also exhibited by $Q = 3H\delta(\rho_{dm} - \rho_{de})$. For $Q = 3H\delta(\rho_{dm} + \rho_{de})$, the coupling to dark matter is more prominent than the coupling to dark energy, causing the energy flow to resemble that of $Q = 3H\delta\rho_{dm}$. For all models, the relative interaction strength diminishes during radiation domination at very high redshift.

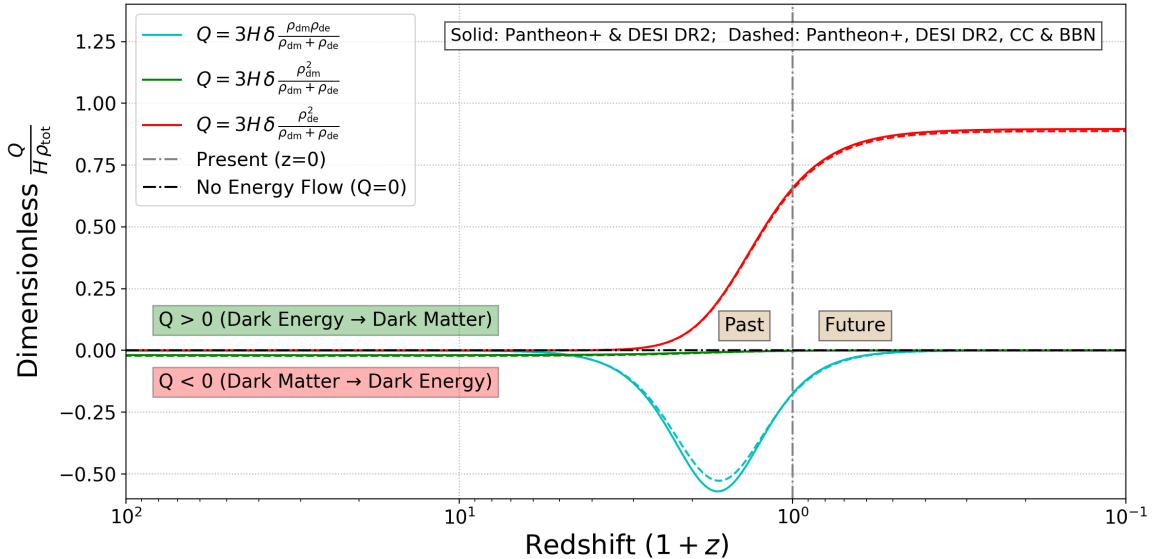


FIG. 5. Direction of energy transfer vs redshift for non-linear interactions, using the mean values obtained in Tables IV and V. The direction of energy transfer is also summarised in Table VII. For $Q = 3H\delta\left(\frac{\rho_{dm}\rho_{de}}{\rho_{dm} + \rho_{de}}\right)$ and $Q = 3H\delta\left(\frac{\rho_{de}^2}{\rho_{dm} + \rho_{de}}\right)$, the relative interaction strength diminishes at high redshift, when dark energy provides only a small contribution to the total energy density. Similarly, for $Q = 3H\delta\left(\frac{\rho_{dm}\rho_{de}}{\rho_{dm} + \rho_{de}}\right)$ and $Q = 3H\delta\left(\frac{\rho_{dm}^2}{\rho_{dm} + \rho_{de}}\right)$, which both involve energy transfer from dark matter to dark energy, the interaction becomes weaker in the future as the dark matter density becomes negligible.

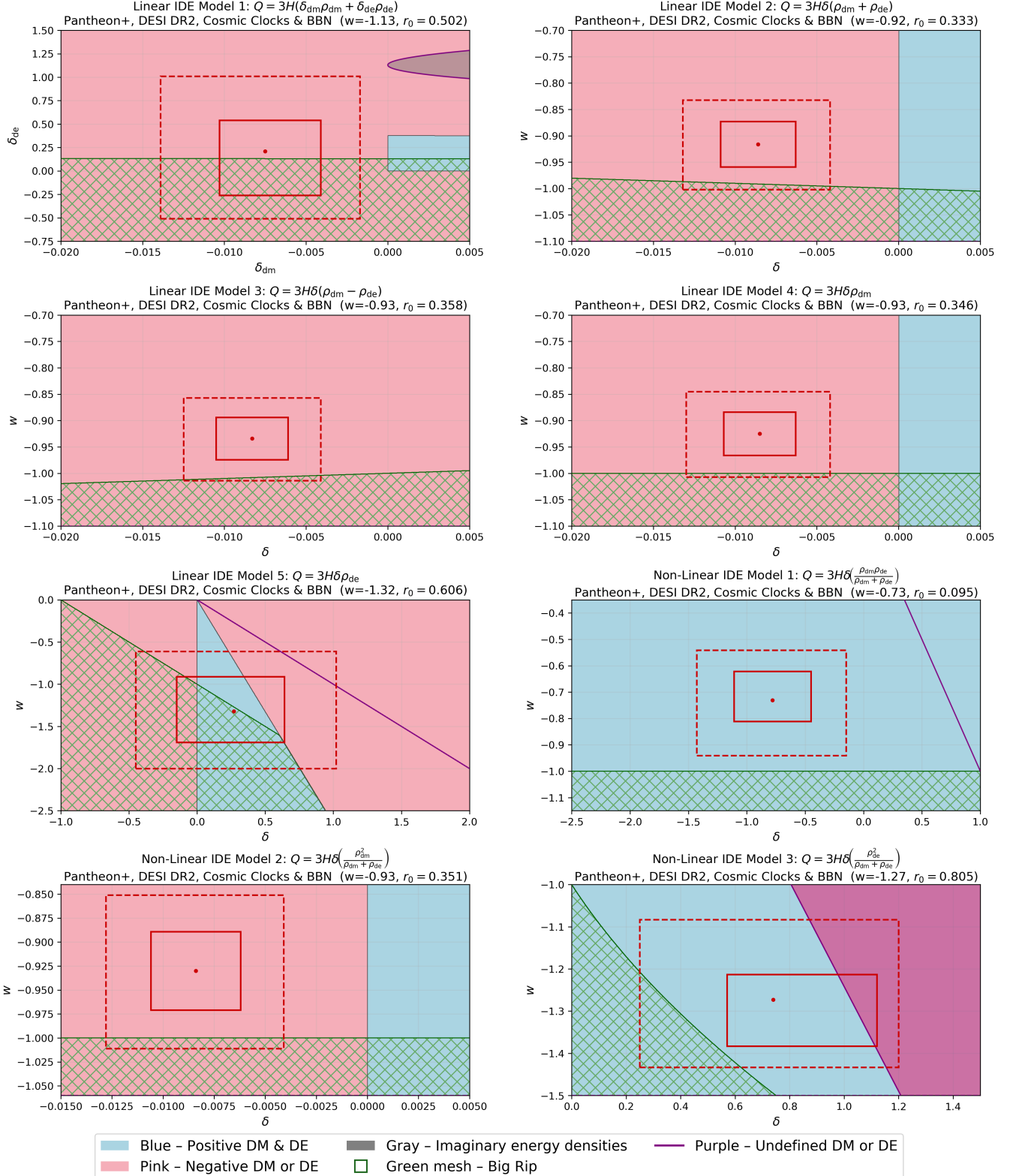


FIG. 6. 2D portraits showing the mean values obtained from Pantheon+, DESI DR2, Cosmic Clocks & BBN data, as reported in Tables IV and V, and how they correspond to the parameter space of each of the eight IDE models, using Tables I and II. The red solid, dashed, and dotted lines indicate the 68% and 95% confidence intervals. Blue areas indicate regions where the model has positive energy densities throughout the entire cosmic evolution. Pink areas indicate that negative energy densities occur either in the past or in the future. The gray overlay indicates the presence of imaginary energy densities, while the purple areas show undefined energy densities. Lastly, the green mesh indicates the presence of future big rip singularities. The purple areas in the bottom-right panel may have undefined values at some scale factor, but this is not guaranteed; see the conditions in Table I.

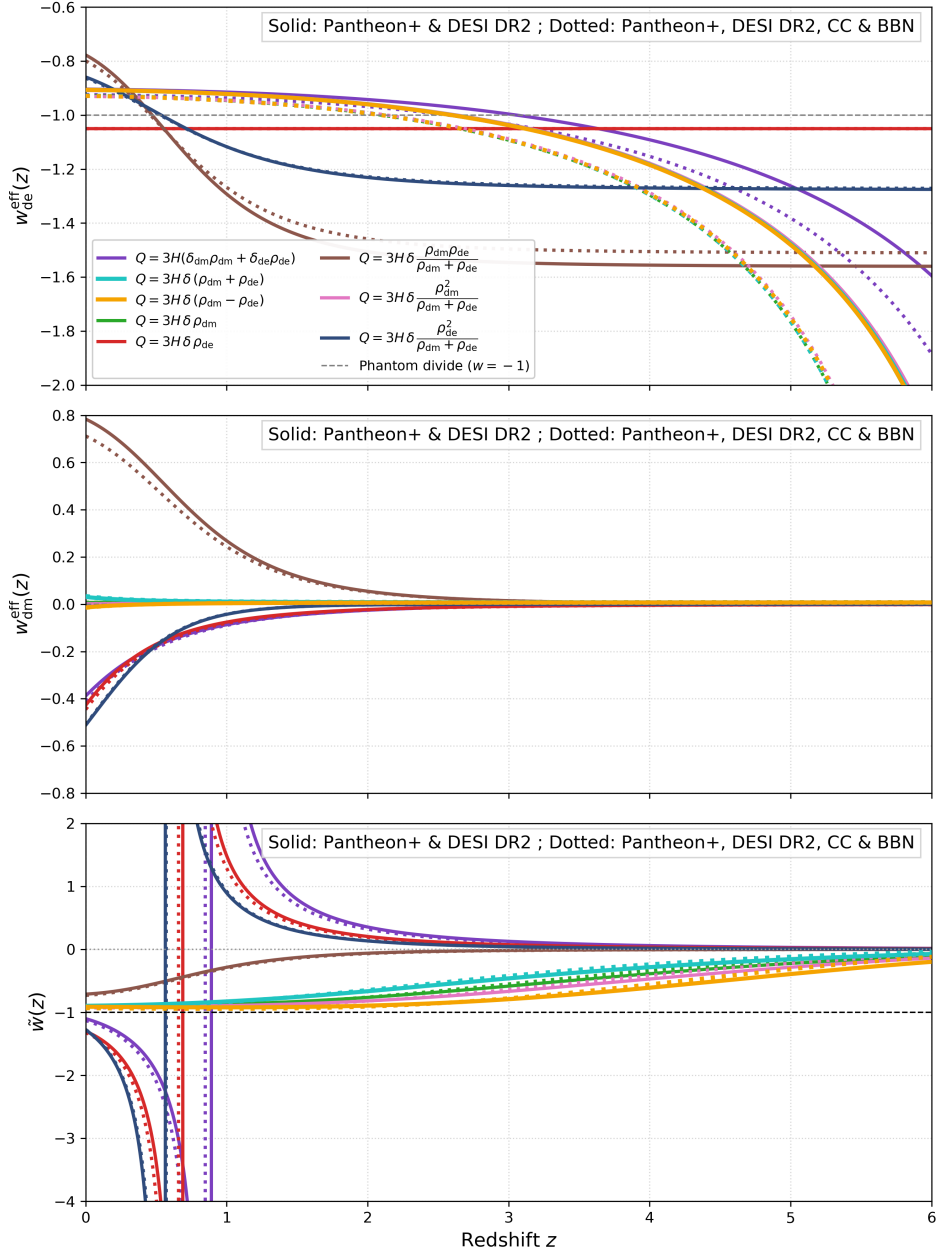


FIG. 7. Evolution of the effective dark energy and dark matter equations of state, $w_{\text{de}}^{\text{eff}}(z)$ and $w_{\text{dm}}^{\text{eff}}(z)$, from (9) (top and middle panels), and the reconstructed dark energy equation of state $\tilde{w}(z)$ from (11) (bottom panel), using the mean values reported in Tables IV and V. In the top panel, phantom-crossing behaviour, where the dark energy density decreases ($w_{\text{de}}^{\text{eff}} > -1$) at low redshift and increases ($w_{\text{de}}^{\text{eff}} < -1$) at higher redshift, is observed in seven of the eight models, with the only exception being $Q = 3H\delta\rho_{\text{de}}$, which has a constant $w_{\text{de}}^{\text{eff}}$ [150]. The curves corresponding to $Q = 3H\delta(\rho_{\text{dm}} + \rho_{\text{de}})$, $Q = 3H\delta(\rho_{\text{dm}} - \rho_{\text{de}})$, $Q = 3H\delta\rho_{\text{dm}}$, and $Q = 3H\delta\left(\frac{\rho_{\text{dm}}^2}{\rho_{\text{dm}} + \rho_{\text{de}}}\right)$ lie almost exactly on top of each other and are nearly indistinguishable. These four models, together with $Q = 3H(\delta_{\text{dm}}\rho_{\text{dm}} + \delta_{\text{de}}\rho_{\text{de}})$, exhibit energy flow from dark matter to dark energy at high redshift and therefore undergo an additional divergent phantom crossing when the dark energy density becomes negative, as discussed in [150, 151]. In the middle panel, the same four models remain nearly indistinguishable and stay close to $w_{\text{dm}}^{\text{eff}} \simeq 0$, preserving cold dark matter behaviour. Models with $Q \propto \rho_{\text{de}}$ and energy flow from dark energy to dark matter at low redshift, namely $Q = 3H(\delta_{\text{dm}}\rho_{\text{dm}} + \delta_{\text{de}}\rho_{\text{de}})$, $Q = 3H\delta\rho_{\text{de}}$, and $Q = 3H\delta\left(\frac{\rho_{\text{de}}^2}{\rho_{\text{dm}} + \rho_{\text{de}}}\right)$, exhibit $w_{\text{dm}}^{\text{eff}} < 0$. Conversely, when energy flows from dark matter to dark energy at low redshift, specifically for $Q = 3H\delta\left(\frac{\rho_{\text{dm}}\rho_{\text{de}}}{\rho_{\text{dm}} + \rho_{\text{de}}}\right)$ and $Q = 3H\delta(\rho_{\text{dm}} - \rho_{\text{de}})$, one finds $w_{\text{dm}}^{\text{eff}} > 0$. In the bottom panel, divergent behaviour of $\tilde{w}(z)$ is observed when energy flows from dark energy to dark matter, as indicated in Figures 4 and 5 and summarized in Table VII, in agreement with the discussion in [151].

Interaction Q	Sign of Q	Sign of $(1+w)$	Sign of ρ_{de}	A priori stable ($\mathbf{d} < 0$)
$3H(\delta_{\text{dm}}\rho_{\text{dm}} + \delta_{\text{de}}\rho_{\text{de}})$	-	-	-	✓
$3H\delta(\rho_{\text{dm}} + \rho_{\text{de}})$	-	+	-	X
$3H\delta(\rho_{\text{dm}} - \rho_{\text{de}})$	-	+	-	X
$3H\delta\rho_{\text{dm}}$	-	+	-	X
$3H\delta\rho_{\text{de}}$	+	-	+	✓
$3H\delta\left(\frac{\rho_{\text{dm}}\rho_{\text{de}}}{\rho_{\text{dm}} + \rho_{\text{de}}}\right)$	-	+	+	✓
$3H\delta\left(\frac{\rho_{\text{dm}}^2}{\rho_{\text{dm}} + \rho_{\text{de}}}\right)$	-	+	-	X
$3H\delta\left(\frac{\rho_{\text{de}}^2}{\rho_{\text{dm}} + \rho_{\text{de}}}\right)$	+	+	+	X

TABLE VIII. Summary of the inferred stability for each interaction from the doom-factor analysis, using the sign of \mathbf{d} in equation (8), based on the posteriors obtained in Tables IV and V. The sign of each quantity is evaluated at early times, or equivalently at high redshift. It should be noted that, since not all parameters are well constrained, alternative possibilities are still allowed.

considered belong to a class of phenomenological interacting dark energy models for which analytical solutions for the dark matter and dark energy densities, and consequently for the Hubble parameter $H(z)$, have been derived in [150, 151]. These include five linear IDE models, namely the most general case $Q = 3H(\delta_{\text{dm}}\rho_{\text{dm}} + \delta_{\text{de}}\rho_{\text{de}})$ and four special cases: $Q = 3H\delta(\rho_{\text{dm}} + \rho_{\text{de}})$, $Q = 3H\delta(\rho_{\text{dm}} - \rho_{\text{de}})$, $Q = 3H\delta\rho_{\text{dm}}$, and $Q = 3H\delta\rho_{\text{de}}$. In addition, we studied three non-linear IDE models: $Q = 3H\delta\left(\frac{\rho_{\text{dm}}\rho_{\text{de}}}{\rho_{\text{dm}} + \rho_{\text{de}}}\right)$, $Q = 3H\delta\left(\frac{\rho_{\text{dm}}^2}{\rho_{\text{dm}} + \rho_{\text{de}}}\right)$, and $Q = 3H\delta\left(\frac{\rho_{\text{de}}^2}{\rho_{\text{dm}} + \rho_{\text{de}}}\right)$.

For all eight IDE models, we find a better fit than ΛCDM from a $\Delta\chi^2$ analysis for both combinations of datasets considered, as shown in Table VI. When using the Akaike Information Criterion (ΔAIC), we find a similarly improved fit in all cases except for $Q = 3H\delta\rho_{\text{de}}$ when Cosmic Clocks and BBN data are added. In all cases, the improvement is largest when using only Pantheon+ and DESI DR2 data, and slightly diminishes when Cosmic Clocks and BBN are included. We also find that models in which $Q \propto \rho_{\text{dm}}$ in any form exhibit the strongest statistical preference, and are accompanied by tighter constraints on δ_{dm} or δ . In contrast, models with $Q \propto \rho_{\text{de}}$, specifically $Q = 3H\delta\rho_{\text{de}}$ and $Q = 3H\delta\left(\frac{\rho_{\text{de}}^2}{\rho_{\text{dm}} + \rho_{\text{de}}}\right)$, show a weaker preference and significantly larger uncertainties on δ_{de} or δ .

In terms of the direction of energy transfer, our analysis shows a preference for sign-switching interactions, with energy transfer from dark energy to dark matter at low redshift and from dark matter to dark energy at higher redshift, in agreement with recent reconstructions [207, 217]. Models that do not allow sign-changing behaviour instead show a preference for energy flow from dark matter to dark energy for all cases in which $Q \propto \rho_{\text{dm}}$ in any form, with the exceptions of $Q = 3H\delta\rho_{\text{de}}$ and $Q = 3H\delta\left(\frac{\rho_{\text{de}}^2}{\rho_{\text{dm}} + \rho_{\text{de}}}\right)$, which instead exhibit energy flow from dark energy to dark matter. These results are illustrated in Figures 4 and 5, and summarized in Table VII. Caution is required when interpreting these findings, since all models that exhibit energy transfer from dark matter to dark energy, except $Q = 3H\delta\left(\frac{\rho_{\text{dm}}\rho_{\text{de}}}{\rho_{\text{dm}} + \rho_{\text{de}}}\right)$, which always produces positive energy densities, are accompanied by negative dark energy densities in the past, which may be physically problematic (see Figure 6 and Table VII). It may nevertheless be argued that negative dark energy does not necessarily constitute a pathology, since the total dark sector remains conserved and positive. In this sense, a unified dark fluid (UDF) description of interacting dark energy models may reproduce the same expansion history while avoiding the apparent pathologies of a two-fluid description. This possibility deserves further investigation and will be explored in future work; connections between UDF and IDE models can already be found in [128, 274, 289–291]. Alternatively, negative energy densities may simply indicate that the phenomenological models considered here are being extrapolated beyond their domain of applicability.

Furthermore, for all interactions considered, we find a phantom-divide crossing in the effective dark energy equation of state $w_{\text{de}}^{\text{eff}}(z)$, with dark energy decreasing ($w_{\text{de}}^{\text{eff}} > -1$) at present and at low redshift, and increasing ($w_{\text{de}}^{\text{eff}} < -1$) at higher redshift in the more distant past. This behaviour is illustrated, together with the evolution of $w_{\text{dm}}^{\text{eff}}(z)$ and $\tilde{w}(z)$, in Figure 7. Divergent behaviour of $w_{\text{de}}^{\text{eff}}(z)$ is not shown in the figure, but is also expected at higher redshift when $\rho_{\text{de}} = 0$, before crossing into negative values. It should be kept in mind that these results are illustrative rather than definitive, since the plots are constructed using only the mean values of the posterior distributions. Different conclusions may therefore be drawn when exploring other regions of the parameter space allowed by the uncertainties.

A quick comparison of the eight models in Tables VII and VIII shows that $Q = 3H\delta\left(\frac{\rho_{\text{dm}}\rho_{\text{de}}}{\rho_{\text{dm}} + \rho_{\text{de}}}\right)$ and $Q = 3H\delta\rho_{\text{de}}$ are the least problematic cases, as both models avoid negative energy densities and early-time instabilities. There is an additional theoretical preference for $Q = 3H\delta\rho_{\text{de}}$, since energy transfer from dark energy to dark matter is favoured by thermodynamic arguments [221]. However, this model also exhibits the weakest statistical performance, as shown

in Table VI.

In conclusion, our analysis shows that interacting dark energy models are promising but also challenging. While these models can fit the data well and provide a possible mechanism for dynamical dark energy, an increasingly topical subject, they are accompanied by a complex parameter space. In several cases, alleviating existing tensions comes at the expense of introducing more severe issues, such as negative energy densities and early-time instabilities. We therefore believe that these models warrant further investigation, extending the analysis to include perturbations, early-time datasets, and interaction models that go beyond purely phenomenological descriptions toward a more robust microphysical foundation.

ACKNOWLEDGMENTS

EDV is supported by a Royal Society Dorothy Hodgkin Research Fellowship. This article is based upon work from the COST Action CA21136 - “Addressing observational tensions in cosmology with systematics and fundamental physics (CosmoVerse)”, supported by COST - “European Cooperation in Science and Technology”.

-
- [1] M. Abdul Karim *et al.* (DESI), DESI DR2 results. II. Measurements of baryon acoustic oscillations and cosmological constraints, *Phys. Rev. D* **112**, 083515 (2025), arXiv:2503.14738 [astro-ph.CO].
- [2] M. Abdul Karim *et al.* (DESI), DESI DR2 results. I. Baryon acoustic oscillations from the Lyman alpha forest, *Phys. Rev. D* **112**, 083514 (2025), arXiv:2503.14739 [astro-ph.CO].
- [3] K. Bechtol *et al.* (DES), Dark Energy Survey Year 6 Results: Photometric Data Set for Cosmology, arXiv preprint (2025), arXiv:2501.05739 [astro-ph.CO].
- [4] N. Aghanim *et al.* (Planck), Planck 2018 results. VI. Cosmological parameters, *Astron. Astrophys.* **641**, A6 (2020), [Erratum: *Astron. Astrophys.* 652, C4 (2021)], arXiv:1807.06209 [astro-ph.CO].
- [5] D. Brout *et al.*, The Pantheon+ Analysis: Cosmological Constraints, *Astrophys. J.* **938**, 110 (2022), arXiv:2202.04077 [astro-ph.CO].
- [6] B. Popovic *et al.* (DES), The Dark Energy Survey Supernova Program: A Reanalysis Of Cosmology Results And Evidence For Evolving Dark Energy With An Updated Type Ia Supernova Calibration (2025), arXiv:2511.07517 [astro-ph.CO].
- [7] J. Martin, Everything You Always Wanted To Know About The Cosmological Constant Problem (But Were Afraid To Ask), *Comptes Rendus Physique* **13**, 566 (2012), arXiv:1205.3365 [astro-ph.CO].
- [8] S. Weinberg, The Cosmological Constant Problem, *Rev. Mod. Phys.* **61**, 1 (1989).
- [9] I. Zlatev, L.-M. Wang, and P. J. Steinhardt, Quintessence, cosmic coincidence, and the cosmological constant, *Phys. Rev. Lett.* **82**, 896 (1999), arXiv:astro-ph/9807002.
- [10] H. E. S. Velten, R. F. vom Marttens, and W. Zimdahl, Aspects of the cosmological “coincidence problem”, *Eur. Phys. J. C* **74**, 3160 (2014), arXiv:1410.2509 [astro-ph.CO].
- [11] L. Verde, T. Treu, and A. G. Riess, Tensions between the Early and the Late Universe, *Nature Astron.* **3**, 891 (2019), arXiv:1907.10625 [astro-ph.CO].
- [12] E. Di Valentino *et al.*, Snowmass2021 - Letter of interest cosmology intertwined II: The hubble constant tension, *Astropart. Phys.* **131**, 102605 (2021), arXiv:2008.11284 [astro-ph.CO].
- [13] E. Di Valentino, O. Mena, S. Pan, L. Visinelli, W. Yang, A. Melchiorri, D. F. Mota, A. G. Riess, and J. Silk, In the realm of the Hubble tension—a review of solutions, *Class. Quant. Grav.* **38**, 153001 (2021), arXiv:2103.01183 [astro-ph.CO].
- [14] L. Perivolaropoulos and F. Skara, Challenges for Λ CDM: An update, *New Astron. Rev.* **95**, 101659 (2022), arXiv:2105.05208 [astro-ph.CO].
- [15] N. Schöneberg, G. Franco Abellán, A. Pérez Sánchez, S. J. Witte, V. Poulin, and J. Lesgourgues, The H0 Olympics: A fair ranking of proposed models, *Phys. Rept.* **984**, 1 (2022), arXiv:2107.10291 [astro-ph.CO].
- [16] P. Shah, P. Lemos, and O. Lahav, A buyer’s guide to the Hubble constant, *Astron. Astrophys. Rev.* **29**, 9 (2021), arXiv:2109.01161 [astro-ph.CO].
- [17] E. Abdalla *et al.*, Cosmology intertwined: A review of the particle physics, astrophysics, and cosmology associated with the cosmological tensions and anomalies, *JHEAp* **34**, 49 (2022), arXiv:2203.06142 [astro-ph.CO].
- [18] E. Di Valentino, Challenges of the Standard Cosmological Model, *Universe* **8**, 399 (2022).
- [19] M. Kamionkowski and A. G. Riess, The Hubble Tension and Early Dark Energy, *Ann. Rev. Nucl. Part. Sci.* **73**, 153 (2023), arXiv:2211.04492 [astro-ph.CO].
- [20] W. Giarè, CMB Anomalies and the Hubble Tension (2023), arXiv:2305.16919 [astro-ph.CO].
- [21] J.-P. Hu and F.-Y. Wang, Hubble Tension: The Evidence of New Physics, *Universe* **9**, 94 (2023), arXiv:2302.05709 [astro-ph.CO].
- [22] L. Verde, N. Schöneberg, and H. Gil-Marín, A tale of many H_0 (2023), arXiv:2311.13305 [astro-ph.CO].
- [23] E. Di Valentino and D. Brout, eds., *The Hubble Constant Tension*, Springer Series in Astrophysics and Cosmology (Springer, 2024).

- [24] E. Di Valentino *et al.* (CosmoVerse), The CosmoVerse White Paper: Addressing observational tensions in cosmology with systematics and fundamental physics (2025), arXiv:2504.01669 [astro-ph.CO].
- [25] D. D. Y. Ong and W. Handley, **unimpeded**: A Public Grid of Nested Sampling Chains for Cosmological Model Comparison and Tension Analysis (2025), arXiv:2511.04661 [astro-ph.CO].
- [26] T. Louis *et al.* (ACT), The Atacama Cosmology Telescope: DR6 Power Spectra, Likelihoods and Λ CDM Parameters (2025), arXiv:2503.14452 [astro-ph.CO].
- [27] E. Camphuis *et al.* (SPT-3G), SPT-3G D1: CMB temperature and polarization power spectra and cosmology from 2019 and 2020 observations of the SPT-3G Main field, arXiv preprint (2025), arXiv:2506.20707 [astro-ph.CO].
- [28] S. Casertano *et al.* (H0DN), The Local Distance Network: a community consensus report on the measurement of the Hubble constant at 1% precision (2025), arXiv:2510.23823 [astro-ph.CO].
- [29] A. Porredon *et al.*, DESI-DR1 3×2 -pt analysis: consistent cosmology across weak lensing surveys (2025), arXiv:2512.15960 [astro-ph.CO].
- [30] E. Di Valentino, A. Melchiorri, and J. Silk, Cosmological hints of modified gravity?, *Phys. Rev. D* **93**, 023513 (2016), arXiv:1509.07501 [astro-ph.CO].
- [31] M. Zumalacarregui, Gravity in the Era of Equality: Towards solutions to the Hubble problem without fine-tuned initial conditions, *Phys. Rev. D* **102**, 023523 (2020), arXiv:2003.06396 [astro-ph.CO].
- [32] S. D. Odintsov, D. Sáez-Chillón Gómez, and G. S. Sharov, Analyzing the H_0 tension in $F(R)$ gravity models, *Nucl. Phys. B* **966**, 115377 (2021), arXiv:2011.03957 [gr-qc].
- [33] T. Adi and E. D. Kovetz, Can conformally coupled modified gravity solve the Hubble tension?, *Phys. Rev. D* **103**, 023530 (2021), arXiv:2011.13853 [astro-ph.CO].
- [34] A. De Felice, S. Mukohyama, and M. C. Pookkillath, Addressing H_0 tension by means of VCDM, *Phys. Lett. B* **816**, 136201 (2021), [Erratum: *Phys. Lett. B* 818, 136364 (2021)], arXiv:2009.08718 [astro-ph.CO].
- [35] L. Pogosian, M. Raveri, K. Koyama, M. Martinelli, A. Silvestri, G.-B. Zhao, J. Li, S. Peirone, and A. Zucca, Imprints of cosmological tensions in reconstructed gravity, *Nature Astron.* **6**, 1484 (2022), arXiv:2107.12992 [astro-ph.CO].
- [36] Y. Akrami *et al.* (CANTATA), *Modified Gravity and Cosmology. An Update by the CANTATA Network*, edited by E. N. Saridakis, R. Lazkoz, V. Salzano, P. Vargas Moniz, S. Capozziello, J. Beltrán Jiménez, M. De Laurentis, and G. J. Olmo (Springer, 2021) arXiv:2105.12582 [gr-qc].
- [37] T. Schiavone, G. Montani, and F. Bombacigno, f(R) gravity in the Jordan frame as a paradigm for the Hubble tension, *Mon. Not. Roy. Astron. Soc.* **522**, L72 (2023), arXiv:2211.16737 [gr-qc].
- [38] M. Ishak *et al.*, Modified Gravity Constraints from the Full Shape Modeling of Clustering Measurements from DESI 2024 (2024), arXiv:2411.12026 [astro-ph.CO].
- [39] E. Specogna, E. Di Valentino, J. Levi Said, and N.-M. Nguyen, Exploring the growth index γ_L : Insights from different CMB dataset combinations and approaches, *Phys. Rev. D* **109**, 043528 (2024), arXiv:2305.16865 [astro-ph.CO].
- [40] E. Specogna, W. Giarè, and E. Di Valentino, Planck-PR4 anisotropy spectra show (better) consistency with General Relativity (2024), arXiv:2411.03896 [astro-ph.CO].
- [41] E. Calabrese *et al.* (Atacama Cosmology Telescope), The Atacama Cosmology Telescope: DR6 constraints on extended cosmological models, *JCAP* **11**, 063, arXiv:2503.14454 [astro-ph.CO].
- [42] W. Giarè, O. Mena, E. Specogna, and E. Di Valentino, Neutrino mass tension or suppressed growth rate of matter perturbations? (2025), arXiv:2507.01848 [astro-ph.CO].
- [43] Y. Tiwari, B. Ghosh, and R. K. Jain, Towards a possible solution to the Hubble tension with Horndeski gravity, *Eur. Phys. J. C* **84**, 220 (2024), arXiv:2301.09382 [astro-ph.CO].
- [44] M. Höglås and E. Mörtsell, Hubble tension and fifth forces, *Phys. Rev. D* **108**, 124050 (2023), arXiv:2309.01744 [astro-ph.CO].
- [45] R. Y. Wen, L. T. Hergt, N. Afshordi, and D. Scott, A cosmic glitch in gravity, *JCAP* **03**, 045, arXiv:2311.03028 [astro-ph.CO].
- [46] C. Pitrou and J.-P. Uzan, Hubble Tension as a Window on the Gravitation of the Dark Matter Sector, *Phys. Rev. Lett.* **132**, 191001 (2024), arXiv:2312.12493 [astro-ph.CO].
- [47] G. Montani, N. Carlevaro, L. A. Escamilla, and E. Di Valentino, Kinetic model for dark energy—dark matter interaction: Scenario for the hubble tension, *Phys. Dark Univ.* **48**, 101848 (2025), arXiv:2404.15977 [gr-qc].
- [48] S. Dwivedi and M. Höglås, 2D BAO vs 3D BAO: solving the Hubble tension with alternative cosmological models (2024), arXiv:2407.04322 [astro-ph.CO].
- [49] O. Akarsu, A. De Felice, E. Di Valentino, S. Kumar, R. C. Nunes, E. Ozulker, J. A. Vazquez, and A. Yadav, Λ_s CDM cosmology from a type-II minimally modified gravity (2024), arXiv:2402.07716 [astro-ph.CO].
- [50] O. Akarsu, B. Bulduk, A. De Felice, N. Katirci, and N. M. Uzun, Unexplored regions in teleparallel f(T) gravity: Sign-changing dark energy density, *Phys. Rev. D* **112**, 083532 (2025), arXiv:2410.23068 [gr-qc].
- [51] M. Höglås and E. Mörtsell, Bimetric gravity improves the fit to DESI BAO and eases the Hubble tension, *Phys. Rev. D* **112**, 103515 (2025), arXiv:2507.03743 [astro-ph.CO].
- [52] K. Lodha *et al.* (DESI), Extended dark energy analysis using DESI DR2 BAO measurements, *Phys. Rev. D* **112**, 083511 (2025), arXiv:2503.14743 [astro-ph.CO].
- [53] A. G. Adame *et al.* (DESI), DESI 2024 VI: cosmological constraints from the measurements of baryon acoustic oscillations, *JCAP* **02**, 021, arXiv:2404.03002 [astro-ph.CO].
- [54] M. Cortês and A. R. Liddle, Interpreting DESI's evidence for evolving dark energy, *JCAP* **12**, 007, arXiv:2404.08056 [astro-ph.CO].
- [55] D. Shlivko and P. J. Steinhardt, Assessing observational constraints on dark energy, *Phys. Lett. B* **855**, 138826 (2024),

- arXiv:2405.03933 [astro-ph.CO].
- [56] O. Luongo and M. Muccino, Model-independent cosmographic constraints from DESI 2024, *Astron. Astrophys.* **690**, A40 (2024), arXiv:2404.07070 [astro-ph.CO].
- [57] I. D. Gialamas, G. Hütsi, K. Kannike, A. Racioppi, M. Raidal, M. Vasar, and H. Veermäe, Interpreting DESI 2024 BAO: late-time dynamical dark energy or a local effect? (2024), arXiv:2406.07533 [astro-ph.CO].
- [58] B. R. Dinda, A new diagnostic for the null test of dynamical dark energy in light of DESI 2024 and other BAO data, *JCAP* **09**, 062, arXiv:2405.06618 [astro-ph.CO].
- [59] M. Najafi, S. Pan, E. Di Valentino, and J. T. Firouzjaee, Dynamical dark energy confronted with multiple CMB missions, *Phys. Dark Univ.* **45**, 101539 (2024), arXiv:2407.14939 [astro-ph.CO].
- [60] H. Wang and Y.-S. Piao, Dark energy in light of recent DESI BAO and Hubble tension (2024), arXiv:2404.18579 [astro-ph.CO].
- [61] G. Ye, M. Martinelli, B. Hu, and A. Silvestri, Hints of Nonminimally Coupled Gravity in DESI 2024 Baryon Acoustic Oscillation Measurements, *Phys. Rev. Lett.* **134**, 181002 (2025), arXiv:2407.15832 [astro-ph.CO].
- [62] Y. Tada and T. Terada, Quintessential interpretation of the evolving dark energy in light of DESI observations, *Phys. Rev. D* **109**, L121305 (2024), arXiv:2404.05722 [astro-ph.CO].
- [63] Y. Carloni, O. Luongo, and M. Muccino, Does dark energy really revive using DESI 2024 data?, *Phys. Rev. D* **111**, 023512 (2025), arXiv:2404.12068 [astro-ph.CO].
- [64] C.-G. Park, J. de Cruz Pérez, and B. Ratra, Using non-DESI data to confirm and strengthen the DESI 2024 spatially flat w_0w_a CDM cosmological parametrization result, *Phys. Rev. D* **110**, 123533 (2024), arXiv:2405.00502 [astro-ph.CO].
- [65] K. Lodha *et al.* (DESI), DESI 2024: Constraints on physics-focused aspects of dark energy using DESI DR1 BAO data, *Phys. Rev. D* **111**, 023532 (2025), arXiv:2405.13588 [astro-ph.CO].
- [66] S. Bhattacharya, G. Borghetto, A. Malhotra, S. Parameswaran, G. Tasinato, and I. Zavala, Cosmological constraints on curved quintessence, *JCAP* **09**, 073, arXiv:2405.17396 [astro-ph.CO].
- [67] O. F. Ramadan, J. Sakstein, and D. Rubin, DESI constraints on exponential quintessence, *Phys. Rev. D* **110**, L041303 (2024), arXiv:2405.18747 [astro-ph.CO].
- [68] S. Pourojaghi, M. Malekjani, and Z. Davari, Cosmological constraints on dark energy parametrizations after DESI 2024: Persistent deviation from standard Λ CDM cosmology (2024), arXiv:2407.09767 [astro-ph.CO].
- [69] W. Giarè, M. Najafi, S. Pan, E. Di Valentino, and J. T. Firouzjaee, Robust preference for Dynamical Dark Energy in DESI BAO and SN measurements, *JCAP* **10**, 035, arXiv:2407.16689 [astro-ph.CO].
- [70] J. a. Rebouças, D. H. F. de Souza, K. Zhong, V. Miranda, and R. Rosenfeld, Investigating late-time dark energy and massive neutrinos in light of DESI Y1 BAO, *JCAP* **02**, 024, arXiv:2408.14628 [astro-ph.CO].
- [71] W. Giarè, Dynamical Dark Energy Beyond Planck? Constraints from multiple CMB probes, DESI BAO and Type-Ia Supernovae (2024), arXiv:2409.17074 [astro-ph.CO].
- [72] C.-G. Park, J. de Cruz Perez, and B. Ratra, Is the w_0w_a CDM cosmological parameterization evidence for dark energy dynamics partially caused by the excess smoothing of Planck CMB anisotropy data? (2024), arXiv:2410.13627 [astro-ph.CO].
- [73] T.-N. Li, Y.-H. Li, G.-H. Du, P.-J. Wu, L. Feng, J.-F. Zhang, and X. Zhang, Revisiting holographic dark energy after DESI 2024 (2024), arXiv:2411.08639 [astro-ph.CO].
- [74] J.-Q. Jiang, D. Pedrotti, S. S. da Costa, and S. Vagnozzi, Non-parametric late-time expansion history reconstruction and implications for the Hubble tension in light of DESI (2024), arXiv:2408.02365 [astro-ph.CO].
- [75] S. Roy Choudhury and T. Okumura, Updated Cosmological Constraints in Extended Parameter Space with Planck PR4, DESI Baryon Acoustic Oscillations, and Supernovae: Dynamical Dark Energy, Neutrino Masses, Lensing Anomaly, and the Hubble Tension, *Astrophys. J. Lett.* **976**, L11 (2024), arXiv:2409.13022 [astro-ph.CO].
- [76] C. Li, J. Wang, D. Zhang, E. N. Saridakis, and Y.-F. Cai, Quantum gravity meets DESI: dynamical dark energy in light of the trans-Planckian censorship conjecture, *JCAP* **08**, 041, arXiv:2504.07791 [astro-ph.CO].
- [77] W. J. Wolf, C. García-García, and P. G. Ferreira, Robustness of Dark Energy Phenomenology Across Different Parameterizations (2025), arXiv:2502.04929 [astro-ph.CO].
- [78] A. J. Shajib and J. A. Frieman, Evolving dark energy models: Current and forecast constraints (2025), arXiv:2502.06929 [astro-ph.CO].
- [79] W. Giarè, T. Mahassen, E. Di Valentino, and S. Pan, An overview of what current data can (and cannot yet) say about evolving dark energy, *Phys. Dark Univ.* **48**, 101906 (2025), arXiv:2502.10264 [astro-ph.CO].
- [80] E. Chaussidon *et al.*, Early time solution as an alternative to the late time evolving dark energy with DESI DR2 BAO (2025), arXiv:2503.24343 [astro-ph.CO].
- [81] D. A. Kessler, L. A. Escamilla, S. Pan, and E. Di Valentino, One-parameter dynamical dark energy: Hints for oscillations (2025), arXiv:2504.00776 [astro-ph.CO].
- [82] Y.-H. Pang, X. Zhang, and Q.-G. Huang, The Impact of the Hubble Tension on the Evidence for Dynamical Dark Energy (2025), arXiv:2503.21600 [astro-ph.CO].
- [83] N. Roy, Dynamical dark energy in the light of DESI 2024 data, *Phys. Dark Univ.* **48**, 101912 (2025), arXiv:2406.00634 [astro-ph.CO].
- [84] S. Roy Choudhury, Cosmology in Extended Parameter Space with DESI DR2 BAO: A 2σ + Detection of Non-zero Neutrino Masses with an Update on Dynamical Dark Energy and Lensing Anomaly (2025), arXiv:2504.15340 [astro-ph.CO].
- [85] A. Paliathanasis, Observational constraints on dark energy models with Λ as an equilibrium point, *Phys. Dark Univ.* **48**, 101956 (2025), arXiv:2502.16221 [astro-ph.CO].
- [86] M. Scherer, M. A. Sabogal, R. C. Nunes, and A. De Felice, Challenging Λ CDM: 5σ Evidence for a Dynamical Dark

- Energy Late-Time Transition (2025), arXiv:2504.20664 [astro-ph.CO].
- [87] W. Giarè, Dynamical dark energy beyond Planck? Constraints from multiple CMB probes, DESI BAO, and type-Ia supernovae, *Phys. Rev. D* **112**, 023508 (2025), arXiv:2409.17074 [astro-ph.CO].
- [88] T. Liu, X. Li, and J. Wang, Dynamical Dark Energy in the Crosshairs: A Joint Analysis with DESI, Type Ia Supernovae, and TDCOSMO Constraints, *Astrophys. J.* **988**, 243 (2025), arXiv:2504.21373 [astro-ph.CO].
- [89] E. M. Teixeira, W. Giarè, N. B. Hogg, T. Montandon, A. Poudou, and V. Poulin, Implications of distance duality violation for the H_0 tension and evolving dark energy (2025), arXiv:2504.10464 [astro-ph.CO].
- [90] F. B. M. d. Santos, J. Morais, S. Pan, W. Yang, and E. Di Valentino, A New Window on Dynamical Dark Energy: Combining DESI-DR2 BAO with future Gravitational Wave Observations (2025), arXiv:2504.04646 [astro-ph.CO].
- [91] E. Specogna, S. A. Adil, E. Ozulker, E. Di Valentino, R. C. Nunes, O. Akarsu, and A. A. Sen, Updated Constraints on Omnipotent Dark Energy: A Comprehensive Analysis with CMB and BAO Data (2025), arXiv:2504.17859 [gr-qc].
- [92] M. A. Sabogal and R. C. Nunes, Robust Evidence for Dynamical Dark Energy from DESI Galaxy-CMB Lensing Cross-Correlation and Geometric Probes (2025), arXiv:2505.24465 [astro-ph.CO].
- [93] H. Cheng, E. Di Valentino, L. A. Escamilla, A. A. Sen, and L. Visinelli, Pressure Parametrization of Dark Energy: First and Second-Order Constraints with Latest Cosmological Data (2025), arXiv:2505.02932 [astro-ph.CO].
- [94] L. Herold and T. Karwal, Bayesian and frequentist perspectives agree on dynamical dark energy (2025), arXiv:2506.12004 [astro-ph.CO].
- [95] H. Cheng, E. Di Valentino, and L. Visinelli, Cosmic Strings as Dynamical Dark Energy: Novel Constraints (2025), arXiv:2505.22066 [astro-ph.CO].
- [96] E. Özulker, E. Di Valentino, and W. Giarè, Dark Energy Crosses the Line: Quantifying and Testing the Evidence for Phantom Crossing (2025), arXiv:2506.19053 [astro-ph.CO].
- [97] D. H. Lee, W. Yang, E. Di Valentino, S. Pan, and C. van de Bruck, The Shape of Dark Energy: Constraining Its Evolution with a General Parametrization (2025), arXiv:2507.11432 [astro-ph.CO].
- [98] A. N. Ormondroyd, W. J. Handley, M. P. Hobson, and A. N. Lasenby, Comparison of dynamical dark energy with Λ CDM in light of DESI DR2 (2025), arXiv:2503.17342 [astro-ph.CO].
- [99] E. Silva and R. C. Nunes, Testing Signatures of Phantom Crossing through Full-Shape Galaxy Clustering Analysis (2025), arXiv:2507.13989 [astro-ph.CO].
- [100] M. Ishak and L. Medina-Varela, Is this the fall of the LCDM throne? Evidence for dynamical dark energy rising from combinations of different types of datasets (2025), arXiv:2507.22856 [astro-ph.CO].
- [101] E. Fazzari, W. Giarè, and E. Di Valentino, Cosmographic Footprints of Dynamical Dark Energy (2025), arXiv:2509.16196 [astro-ph.CO].
- [102] A. Smith, E. Özulker, E. Di Valentino, and C. van de Bruck, Dynamical Dark Energy Meets Varying Electron Mass: Implications for Phantom Crossing and the Hubble Constant (2025), arXiv:2510.21931 [astro-ph.CO].
- [103] Z. Zhang, T. Xu, and Y. Chen, Dynamical Dark Energy and the Unresolved Hubble Tension: Multi-model Constraints from DESI 2025 and Other Probes (2025), arXiv:2512.07281 [astro-ph.CO].
- [104] H. Cheng, S. Pan, and E. Di Valentino, Beyond Two Parameters: Revisiting Dark Energy with the Latest Cosmic Probes (2025), arXiv:2512.09866 [astro-ph.CO].
- [105] S. Tulin and H.-B. Yu, Dark Matter Self-interactions and Small Scale Structure, *Phys. Rept.* **730**, 1 (2018), arXiv:1705.02358 [hep-ph].
- [106] M. A. Buen-Abad, G. Marques-Tavares, and M. Schmaltz, Non-Abelian dark matter and dark radiation, *Phys. Rev. D* **92**, 023531 (2015), arXiv:1505.03542 [hep-ph].
- [107] E. Di Valentino, C. Boehm, E. Hivon, and F. R. Bouchet, Reducing the H_0 and σ_8 tensions with Dark Matter-neutrino interactions, *Phys. Rev. D* **97**, 043513 (2018), arXiv:1710.02559 [astro-ph.CO].
- [108] L. A. Anchordoqui, V. Barger, D. Marfatia, and J. F. Soriano, Decay of multiple dark matter particles to dark radiation in different epochs does not alleviate the Hubble tension, *Phys. Rev. D* **105**, 103512 (2022), arXiv:2203.04818 [astro-ph.CO].
- [109] S. Pan, O. Seto, T. Takahashi, and Y. Toda, Constraints on sterile neutrinos and the cosmological tensions, *Phys. Rev. D* **110**, 083524 (2024), arXiv:2312.15435 [astro-ph.CO].
- [110] I. J. Allali, D. Aloni, and N. Schöneberg, Cosmological probes of Dark Radiation from Neutrino Mixing, *JCAP* **09**, 019, arXiv:2404.16822 [astro-ph.CO].
- [111] R. T. Co, N. Fernandez, A. Ghalsasi, K. Harigaya, and J. Shelton, Axion baryogenesis puts a new spin on the Hubble tension, *Phys. Rev. D* **110**, 083534 (2024), arXiv:2405.12268 [hep-ph].
- [112] A. Aboubrahim and P. Nath, Interacting ultralight dark matter and dark energy and fits to cosmological data in a field theory approach, *JCAP* **09**, 076, arXiv:2406.19284 [astro-ph.CO].
- [113] S. Kumar and R. C. Nunes, Probing the interaction between dark matter and dark energy in the presence of massive neutrinos, *Phys. Rev. D* **94**, 123511 (2016), arXiv:1608.02454 [astro-ph.CO].
- [114] R. Murgia, S. Gariazzo, and N. Fornengo, Constraints on the Coupling between Dark Energy and Dark Matter from CMB data, *JCAP* **04**, 014, arXiv:1602.01765 [astro-ph.CO].
- [115] S. Kumar and R. C. Nunes, Echo of interactions in the dark sector, *Phys. Rev. D* **96**, 103511 (2017), arXiv:1702.02143 [astro-ph.CO].
- [116] E. Di Valentino, A. Melchiorri, and O. Mena, Can interacting dark energy solve the H_0 tension?, *Phys. Rev. D* **96**, 043503 (2017), arXiv:1704.08342 [astro-ph.CO].
- [117] S. Kumar, Remedy of some cosmological tensions via effective phantom-like behavior of interacting vacuum energy, *Phys. Dark Univ.* **33**, 100862 (2021), arXiv:2102.12902 [astro-ph.CO].
- [118] L.-Y. Gao, Z.-W. Zhao, S.-S. Xue, and X. Zhang, Relieving the H_0 tension with a new interacting dark energy model,

- JCAP **07**, 005, arXiv:2101.10714 [astro-ph.CO].
- [119] S. Pan and W. Yang, On the interacting dark energy scenarios - the case for Hubble constant tension (2023), arXiv:2310.07260 [astro-ph.CO].
- [120] D. Benisty, S. Pan, D. Staicova, E. Di Valentino, and R. C. Nunes, Late-time constraints on interacting dark energy: Analysis independent of H_0 , rd , and MB , Astron. Astrophys. **688**, A156 (2024), arXiv:2403.00056 [astro-ph.CO].
- [121] W. Yang, E. Di Valentino, O. Mena, S. Pan, and R. C. Nunes, All-inclusive interacting dark sector cosmologies, Phys. Rev. D **101**, 083509 (2020), arXiv:2001.10852 [astro-ph.CO].
- [122] M. Forconi, W. Giarè, O. Mena, Ruchika, E. Di Valentino, A. Melchiorri, and R. C. Nunes, A double take on early and interacting dark energy from JWST, JCAP **05**, 097, arXiv:2312.11074 [astro-ph.CO].
- [123] A. Pourtsidou and T. Tram, Reconciling CMB and structure growth measurements with dark energy interactions, Phys. Rev. D **94**, 043518 (2016), arXiv:1604.04222 [astro-ph.CO].
- [124] E. Di Valentino, A combined analysis of the H_0 late time direct measurements and the impact on the Dark Energy sector, Mon. Not. Roy. Astron. Soc. **502**, 2065 (2021), arXiv:2011.00246 [astro-ph.CO].
- [125] E. Di Valentino and O. Mena, A fake Interacting Dark Energy detection?, Mon. Not. Roy. Astron. Soc. **500**, L22 (2020), arXiv:2009.12620 [astro-ph.CO].
- [126] R. C. Nunes and E. Di Valentino, Dark sector interaction and the supernova absolute magnitude tension, Phys. Rev. D **104**, 063529 (2021), arXiv:2107.09151 [astro-ph.CO].
- [127] W. Yang, A. Mukherjee, E. Di Valentino, and S. Pan, Interacting dark energy with time varying equation of state and the H_0 tension, Phys. Rev. D **98**, 123527 (2018), arXiv:1809.06883 [astro-ph.CO].
- [128] R. von Marttens, L. Lombriser, M. Kunz, V. Marra, L. Casarini, and J. Alcaniz, Dark degeneracy I: Dynamical or interacting dark energy?, Phys. Dark Univ. **28**, 100490 (2020), arXiv:1911.02618 [astro-ph.CO].
- [129] M. Lucca and D. C. Hooper, Shedding light on dark matter-dark energy interactions, Phys. Rev. D **102**, 123502 (2020), arXiv:2002.06127 [astro-ph.CO].
- [130] B. Wang, E. Abdalla, F. Atrio-Barandela, and D. Pavón, Further understanding the interaction between dark energy and dark matter: current status and future directions, Rept. Prog. Phys. **87**, 036901 (2024), arXiv:2402.00819 [astro-ph.CO].
- [131] L.-Y. Gao, S.-S. Xue, and X. Zhang, Dark energy and matter interacting scenario to relieve H_0 and S_8 tensions*, Chin. Phys. C **48**, 051001 (2024), arXiv:2212.13146 [astro-ph.CO].
- [132] Y. Zhai, W. Giarè, C. van de Bruck, E. Di Valentino, O. Mena, and R. C. Nunes, A consistent view of interacting dark energy from multiple CMB probes, JCAP **07**, 032, arXiv:2303.08201 [astro-ph.CO].
- [133] A. Bernui, E. Di Valentino, W. Giarè, S. Kumar, and R. C. Nunes, Exploring the H_0 tension and the evidence for dark sector interactions from 2D BAO measurements, Phys. Rev. D **107**, 103531 (2023), arXiv:2301.06097 [astro-ph.CO].
- [134] N. Becker, D. C. Hooper, F. Kahlhoefer, J. Lesgourgues, and N. Schöneberg, Cosmological constraints on multi-interacting dark matter, JCAP **02**, 019, arXiv:2010.04074 [astro-ph.CO].
- [135] G. A. Hoerning, R. G. Landim, L. O. Ponte, R. P. Rolim, F. B. Abdalla, and E. Abdalla, Constraints on interacting dark energy revisited: implications for the Hubble tension (2023), arXiv:2308.05807 [astro-ph.CO].
- [136] W. Giarè, Y. Zhai, S. Pan, E. Di Valentino, R. C. Nunes, and C. van de Bruck, Tightening the reins on nonminimal dark sector physics: Interacting dark energy with dynamical and nondynamical equation of state, Phys. Rev. D **110**, 063527 (2024), arXiv:2404.02110 [astro-ph.CO].
- [137] L. A. Escamilla, O. Akarsu, E. Di Valentino, and J. A. Vazquez, Model-independent reconstruction of the interacting dark energy kernel: Binned and Gaussian process, JCAP **11**, 051, arXiv:2305.16290 [astro-ph.CO].
- [138] M. A. van der Westhuizen and A. Abebe, Interacting dark energy: clarifying the cosmological implications and viability conditions, JCAP **01**, 048, arXiv:2302.11949 [gr-qc].
- [139] E. Silva, U. Zúñiga Bolaño, R. C. Nunes, and E. Di Valentino, Non-Linear Matter Power Spectrum Modeling in Interacting Dark Energy Cosmologies (2024), arXiv:2403.19590 [astro-ph.CO].
- [140] E. Di Valentino, A. Melchiorri, O. Mena, and S. Vagnozzi, Interacting dark energy in the early 2020s: A promising solution to the H_0 and cosmic shear tensions, Phys. Dark Univ. **30**, 100666 (2020), arXiv:1908.04281 [astro-ph.CO].
- [141] T.-N. Li, P.-J. Wu, G.-H. Du, S.-J. Jin, H.-L. Li, J.-F. Zhang, and X. Zhang, Constraints on Interacting Dark Energy Models from the DESI Baryon Acoustic Oscillation and DES Supernovae Data, Astrophys. J. **976**, 1 (2024), arXiv:2407.14934 [astro-ph.CO].
- [142] N. N. Pooya, Growth of matter perturbations in the interacting dark energy-dark matter scenarios, Phys. Rev. D **110**, 043510 (2024), arXiv:2407.03766 [astro-ph.CO].
- [143] S. Halder, J. de Haro, T. Saha, and S. Pan, Phase space analysis of sign-shifting interacting dark energy models, Phys. Rev. D **109**, 083522 (2024), arXiv:2403.01397 [gr-qc].
- [144] S. Castello, M. Mancarella, N. Grimm, D. Sobral-Blanco, I. Tutzus, and C. Bonvin, Gravitational redshift constraints on the effective theory of interacting dark energy, JCAP **05**, 003, arXiv:2311.14425 [astro-ph.CO].
- [145] Y.-H. Yao and X.-H. Meng, Can interacting dark energy with dynamical coupling resolve the Hubble tension, Phys. Dark Univ. **39**, 101165 (2023).
- [146] K. R. Mishra, S. K. J. Pacif, R. Kumar, and K. Bamba, Cosmological implications of an interacting model of dark matter & dark energy, Phys. Dark Univ. **40**, 101211 (2023), arXiv:2301.08743 [gr-qc].
- [147] R. C. Nunes, S. Pan, and E. N. Saridakis, New constraints on interacting dark energy from cosmic chronometers, Phys. Rev. D **94**, 023508 (2016), arXiv:1605.01712 [astro-ph.CO].
- [148] E. Silva, M. A. Sabogal, M. S. Souza, R. C. Nunes, E. Di Valentino, and S. Kumar, New Constraints on Interacting Dark Energy from DESI DR2 BAO Observations, arXiv preprint (2025), arXiv:2503.23225 [astro-ph.CO].
- [149] W. Yang, S. Zhang, O. Mena, S. Pan, and E. Di Valentino, Dark Energy Is Not That Into You: Variable Couplings after

- DESI DR2 BAO (2025), arXiv:2508.19109 [astro-ph.CO].
- [150] M. van der Westhuizen, A. Abebe, and E. Di Valentino, I. Linear interacting dark energy: Analytical solutions and theoretical pathologies, *Phys. Dark Univ.* **50**, 102119 (2025), arXiv:2509.04495 [gr-qc].
- [151] M. van der Westhuizen, A. Abebe, and E. Di Valentino, II. Non-Linear Interacting Dark Energy: Analytical Solutions and Theoretical Pathologies, *Phys. Dark Univ.* **50**, 102120 (2025), arXiv:2509.04494 [gr-qc].
- [152] M. van der Westhuizen, A. Abebe, and E. Di Valentino, III. Interacting Dark Energy: Summary of models, Pathologies, and Constraints, *Phys. Dark Univ.* **50**, 102121 (2025), arXiv:2509.04496 [gr-qc].
- [153] N. Lee, Y. Ali-Haïmoud, N. Schöneberg, and V. Poulin, What It Takes to Solve the Hubble Tension through Modifications of Cosmological Recombination, *Phys. Rev. Lett.* **130**, 161003 (2023), arXiv:2212.04494 [astro-ph.CO].
- [154] K. L. Greene and F.-Y. Cyr-Racine, Thomson scattering: one rate to rule them all, *JCAP* **10**, 065, arXiv:2306.06165 [astro-ph.CO].
- [155] K. Greene and F.-Y. Cyr-Racine, Ratio-preserving approach to cosmological concordance, *Phys. Rev. D* **110**, 043524 (2024), arXiv:2403.05619 [astro-ph.CO].
- [156] M. Baryakhtar, O. Simon, and Z. J. Weiner, Cosmology with varying fundamental constants from hyperlight, coupled scalars, *Phys. Rev. D* **110**, 083505 (2024), arXiv:2405.10358 [astro-ph.CO].
- [157] O. Seto and Y. Toda, DESI constraints on the varying electron mass model and axionlike early dark energy, *Phys. Rev. D* **110**, 083501 (2024), arXiv:2405.11869 [astro-ph.CO].
- [158] G. P. Lynch, L. Knox, and J. Chluba, DESI observations and the Hubble tension in light of modified recombination, *Phys. Rev. D* **110**, 083538 (2024), arXiv:2406.10202 [astro-ph.CO].
- [159] Y. Toda, W. Giarè, E. Özülker, E. Di Valentino, and S. Vagnozzi, Combining pre- and post-recombination new physics to address cosmological tensions: case study with varying electron mass and a sign-switching cosmological constant (2024), arXiv:2407.01173 [astro-ph.CO].
- [160] N. Schöneberg and L. Vacher, The mass effect – Variations of masses and their impact on cosmology (2024), arXiv:2407.16845 [astro-ph.CO].
- [161] A. Smith, M. Mylova, C. van de Bruck, C. P. Burgess, and E. Di Valentino, The Serendipitous Axiodilaton: A Self-Consistent Recombination-Era Solution to the Hubble Tension (2025), arXiv:2512.13544 [astro-ph.CO].
- [162] V. Poulin, T. L. Smith, T. Karwal, and M. Kamionkowski, Early Dark Energy Can Resolve The Hubble Tension, *Phys. Rev. Lett.* **122**, 221301 (2019), arXiv:1811.04083 [astro-ph.CO].
- [163] T. L. Smith, V. Poulin, and M. A. Amin, Oscillating scalar fields and the Hubble tension: a resolution with novel signatures, *Phys. Rev. D* **101**, 063523 (2020), arXiv:1908.06995 [astro-ph.CO].
- [164] F. Niedermann and M. S. Sloth, New early dark energy, *Phys. Rev. D* **103**, L041303 (2021), arXiv:1910.10739 [astro-ph.CO].
- [165] C. Krishnan, E. Ó. Colgáin, Ruchika, A. A. Sen, M. M. Sheikh-Jabbari, and T. Yang, Is there an early Universe solution to Hubble tension?, *Phys. Rev. D* **102**, 103525 (2020), arXiv:2002.06044 [astro-ph.CO].
- [166] G. Ye, J. Zhang, and Y.-S. Piao, Alleviating both H_0 and S_8 tensions: Early dark energy lifts the CMB-lockdown on ultralight axion, *Phys. Lett. B* **839**, 137770 (2023), arXiv:2107.13391 [astro-ph.CO].
- [167] V. Poulin, T. L. Smith, and A. Bartlett, Dark energy at early times and ACT data: A larger Hubble constant without late-time priors, *Phys. Rev. D* **104**, 123550 (2021), arXiv:2109.06229 [astro-ph.CO].
- [168] F. Niedermann and M. S. Sloth, Hot new early dark energy, *Phys. Rev. D* **105**, 063509 (2022), arXiv:2112.00770 [hep-ph].
- [169] D. H. F. de Souza and R. Rosenfeld, Can neutrino-assisted early dark energy models ameliorate the H_0 tension in a natural way?, *Phys. Rev. D* **108**, 083512 (2023), arXiv:2302.04644 [astro-ph.CO].
- [170] V. Poulin, T. L. Smith, and T. Karwal, The Ups and Downs of Early Dark Energy solutions to the Hubble tension: A review of models, hints and constraints circa 2023, *Phys. Dark Univ.* **42**, 101348 (2023), arXiv:2302.09032 [astro-ph.CO].
- [171] J. S. Cruz, F. Niedermann, and M. S. Sloth, Cold New Early Dark Energy pulls the trigger on the H_0 and S_8 tensions: a simultaneous solution to both tensions without new ingredients, *JCAP* **11**, 033, arXiv:2305.08895 [astro-ph.CO].
- [172] F. Niedermann and M. S. Sloth, New Early Dark Energy as a solution to the H_0 and S_8 tensions (2023), arXiv:2307.03481 [hep-ph].
- [173] S. Vagnozzi, Seven Hints That Early-Time New Physics Alone Is Not Sufficient to Solve the Hubble Tension, *Universe* **9**, 393 (2023), arXiv:2308.16628 [astro-ph.CO].
- [174] G. Efstathiou, E. Rosenberg, and V. Poulin, Improved Planck Constraints on Axionlike Early Dark Energy as a Resolution of the Hubble Tension, *Phys. Rev. Lett.* **132**, 221002 (2024), arXiv:2311.00524 [astro-ph.CO].
- [175] J. L. Cervantes-Cota, S. Galindo-Uriarri, and G. F. Smoot, The Unsettled Number: Hubble's Tension, *Universe* **9**, 501 (2023), arXiv:2311.07552 [physics.hist-ph].
- [176] M. Garny, F. Niedermann, H. Rubira, and M. S. Sloth, Hot new early dark energy bridging cosmic gaps: Supercooled phase transition reconciles stepped dark radiation solutions to the Hubble tension with BBN, *Phys. Rev. D* **110**, 023531 (2024), arXiv:2404.07256 [astro-ph.CO].
- [177] W. Giarè, Inflation, the Hubble tension, and early dark energy: An alternative overview, *Phys. Rev. D* **109**, 123545 (2024), arXiv:2404.12779 [astro-ph.CO].
- [178] W. Giarè, J. Betts, C. van de Bruck, and E. Di Valentino, A model-independent test of pre-recombination New Physics: Machine Learning based estimate of the Sound Horizon from Gravitational Wave Standard Sirens and the Baryon Acoustic Oscillation Angular Scale (2024), arXiv:2406.07493 [astro-ph.CO].
- [179] V. Poulin, T. L. Smith, R. Calderón, and T. Simon, Implications of the cosmic calibration tension beyond H_0 and the synergy between early- and late-time new physics, *Phys. Rev. D* **111**, 083552 (2025), arXiv:2407.18292 [astro-ph.CO].
- [180] D. Pedrotti, J.-Q. Jiang, L. A. Escamilla, S. S. da Costa, and S. Vagnozzi, Multidimensionality of the Hubble tension:

- the roles of Ω_m and ω_c (2024), arXiv:2408.04530 [astro-ph.CO].
- [181] J. Kochappan, L. Yin, B.-H. Lee, and T. Ghosh, Observational evidence for early dark energy as a unified explanation for cosmic birefringence and the Hubble tension, *Phys. Rev. D* **112**, 063562 (2025), arXiv:2408.09521 [astro-ph.CO].
- [182] L. Amendola, Coupled quintessence, *Phys. Rev. D* **62**, 043511 (2000), arXiv:astro-ph/9908023.
- [183] W. Zimdahl and D. Pavon, Interacting quintessence, *Phys. Lett. B* **521**, 133 (2001), arXiv:astro-ph/0105479.
- [184] L. P. Chimento, A. S. Jakubi, D. Pavon, and W. Zimdahl, Interacting quintessence solution to the coincidence problem, *Phys. Rev. D* **67**, 083513 (2003), arXiv:astro-ph/0303145.
- [185] G. R. Farrar and P. J. E. Peebles, Interacting dark matter and dark energy, *Astrophys. J.* **604**, 1 (2004), arXiv:astro-ph/0307316.
- [186] P. Wang and X.-H. Meng, Can vacuum decay in our universe?, *Class. Quant. Grav.* **22**, 283 (2005), arXiv:astro-ph/0408495.
- [187] G. Olivares, F. Atrio-Barandela, and D. Pavon, Matter density perturbations in interacting quintessence models, *Phys. Rev. D* **74**, 043521 (2006), arXiv:astro-ph/0607604.
- [188] H. M. Sadjadi and M. Alimohammadi, Cosmological coincidence problem in interactive dark energy models, *Phys. Rev. D* **74**, 103007 (2006), arXiv:gr-qc/0610080.
- [189] M. Quartin, M. O. Calvao, S. E. Joras, R. R. R. Reis, and I. Waga, Dark Interactions and Cosmological Fine-Tuning, *JCAP* **05**, 007, arXiv:0802.0546 [astro-ph].
- [190] S. del Campo, R. Herrera, and D. Pavon, Interacting models may be key to solve the cosmic coincidence problem, *JCAP* **01**, 020, arXiv:0812.2210 [gr-qc].
- [191] G. Caldera-Cabral, R. Maartens, and L. A. Urena-Lopez, Dynamics of interacting dark energy, *Phys. Rev. D* **79**, 063518 (2009), arXiv:0812.1827 [gr-qc].
- [192] J.-H. He, B. Wang, and E. Abdalla, Testing the interaction between dark energy and dark matter via latest observations, *Phys. Rev. D* **83**, 063515 (2011), arXiv:1012.3904 [astro-ph.CO].
- [193] S. del Campo, R. Herrera, and D. Pavón, Interaction in the dark sector, *Phys. Rev. D* **91**, 123539 (2015), arXiv:1507.00187 [gr-qc].
- [194] M. Califano, I. de Martino, D. Vernieri, and S. Capozziello, Exploiting the Einstein Telescope to solve the Hubble tension, *Phys. Rev. D* **107**, 123519 (2023), arXiv:2208.13999 [astro-ph.CO].
- [195] G. Liu, Z. Zhou, Y. Mu, and L. Xu, Kinetically coupled scalar fields model and cosmological tensions, *Mon. Not. Roy. Astron. Soc.* **529**, 1852 (2024), arXiv:2308.07069 [astro-ph.CO].
- [196] M. A. Sabogal, E. Silva, R. C. Nunes, S. Kumar, and E. Di Valentino, Sign switching in dark sector coupling interactions as a candidate for resolving cosmological tensions, *Phys. Rev. D* **111**, 043531 (2025), arXiv:2501.10323 [astro-ph.CO].
- [197] S. Kumar, R. C. Nunes, and S. K. Yadav, Dark sector interaction: a remedy of the tensions between CMB and LSS data, *Eur. Phys. J. C* **79**, 576 (2019), arXiv:1903.04865 [astro-ph.CO].
- [198] L. A. Anchordoqui, E. Di Valentino, S. Pan, and W. Yang, Dissecting the H0 and S8 tensions with Planck + BAO + supernova type Ia in multi-parameter cosmologies, *JHEAp* **32**, 28 (2021), arXiv:2107.13932 [astro-ph.CO].
- [199] S. Gariazzo, E. Di Valentino, O. Mena, and R. C. Nunes, Late-time interacting cosmologies and the Hubble constant tension, *Phys. Rev. D* **106**, 023530 (2022), arXiv:2111.03152 [astro-ph.CO].
- [200] M. Lucca, Dark energy–dark matter interactions as a solution to the S8 tension, *Phys. Dark Univ.* **34**, 100899 (2021), arXiv:2105.09249 [astro-ph.CO].
- [201] M. A. Sabogal, E. Silva, R. C. Nunes, S. Kumar, E. Di Valentino, and W. Giarè, Quantifying the S8 tension and evidence for interacting dark energy from redshift-space distortion measurements, *Phys. Rev. D* **110**, 123508 (2024), arXiv:2408.12403 [astro-ph.CO].
- [202] G. Liu, Z. Zhou, Y. Mu, and L. Xu, Alleviating cosmological tensions with a coupled scalar fields model, *Phys. Rev. D* **108**, 083523 (2023), arXiv:2307.07228 [astro-ph.CO].
- [203] W. Yang, S. Pan, E. Di Valentino, O. Mena, D. F. Mota, and S. Chakraborty, Probing the cold nature of dark matter, *Phys. Rev. D* **111**, 103509 (2025), arXiv:2504.11973 [astro-ph.CO].
- [204] W. Liu, Y. Wu, S. Pan, and W. Yang, Solving an interacting quintessence model with a sound horizon initial condition and its observational constraints, *JHEAp* **47**, 100403 (2025), arXiv:2507.09258 [gr-qc].
- [205] U. Andrade *et al.* (DESI), Validation of the DESI DR2 Measurements of Baryon Acoustic Oscillations from Galaxies and Quasars, arXiv preprint (2025), arXiv:2503.14742 [astro-ph.CO].
- [206] G. Gu *et al.* (DESI), Dynamical Dark Energy in light of the DESI DR2 Baryonic Acoustic Oscillations Measurements, arXiv preprint 10.1038/s41550-025-02669-6 (2025), arXiv:2504.06118 [astro-ph.CO].
- [207] S. L. Guedezounme, B. R. Dinda, and R. Maartens, Phantom crossing or dark interaction? (2025), arXiv:2507.18274 [astro-ph.CO].
- [208] S. Pan, S. Paul, E. N. Saridakis, and W. Yang, Interacting dark energy after DESI DR2: a challenge for Λ CDM paradigm? (2025), arXiv:2504.00994 [astro-ph.CO].
- [209] R. Shah, P. Mukherjee, and S. Pal, Interacting Dark Sectors in light of DESI DR2, *Mon. Not. Roy. Astron. Soc.* **542**, 2936 (2025), arXiv:2503.21652 [astro-ph.CO].
- [210] M. van der Westhuizen, D. Figueruelo, R. Thubisi, S. Sahlu, A. Abebe, and A. Paliathanasis, Compartmentalization in the dark sector of the universe after DESI DR2 BAO data, *Phys. Dark Univ.* **50**, 102107 (2025), arXiv:2505.23306 [astro-ph.CO].
- [211] W. Giarè, M. A. Sabogal, R. C. Nunes, and E. Di Valentino, Interacting Dark Energy after DESI Baryon Acoustic Oscillation Measurements, *Phys. Rev. Lett.* **133**, 251003 (2024), arXiv:2404.15232 [astro-ph.CO].
- [212] Z. Zhu, Q. Jiang, Y. Liu, P. Wu, and N. Liang, Cosmological Constraints on the Phenomenological Interacting Dark

- Energy Model with Fermi Gamma-Ray Bursts and DESI DR2 (2025), arXiv:2511.16032 [astro-ph.CO].
- [213] M. Gonzalez-Espinoza, R. Herrera, G. Otalora, C. Ríos, and C. Rodriguez-Benites, Cosmological dynamics of interacting dark matter-dark energy in generalized Rastall gravity (2025), arXiv:2511.14089 [gr-qc].
- [214] P. K. MV, N. Kavya, and K. Arun, Spontaneous Symmetry Breaking as a Late-Time Trigger for Interacting Dark Energy (2025), arXiv:2511.14235 [astro-ph.CO].
- [215] Z.-H. Lyu, R.-G. Cai, S.-J. Wang, and X.-X. Zeng, Constraining interacting dark energy models with black hole superradiance (2025), arXiv:2511.16244 [astro-ph.CO].
- [216] P.-J. Wu, M. Zhang, and S.-J. Jin, How Dark Sector Equations of State Govern Interaction Signatures (2025), arXiv:2512.05548 [astro-ph.CO].
- [217] Y.-H. Li and X. Zhang, Cosmic sign-reversal: non-parametric reconstruction of interacting dark energy with DESI DR2, *JCAP* **12**, 018, arXiv:2506.18477 [astro-ph.CO].
- [218] J.-Q. Wang, R.-G. Cai, Z.-K. Guo, and S.-J. Wang, Resolving the Planck-DESI tension by non-minimally coupled quintessence, arXiv preprint (2025), arXiv:2508.01759 [astro-ph.CO].
- [219] Z. Yao, G. Ye, and A. Silvestri, A General Model for Dark Energy Crossing the Phantom Divide, arXiv preprint (2025), arXiv:2508.01378 [gr-qc].
- [220] S. Bhattacharya, G. Borghetto, A. Malhotra, S. Parameswaran, G. Tasinato, and I. Zavala, Cosmological tests of quintessence in quantum gravity, *JCAP* **04**, 086, arXiv:2410.21243 [astro-ph.CO].
- [221] D. Pavon and B. Wang, Le Chatelier-Braun principle in cosmological physics, *Gen. Rel. Grav.* **41**, 1 (2009), arXiv:0712.0565 [gr-qc].
- [222] V. Salvatelli, A. Marchini, L. Lopez-Honorez, and O. Mena, New constraints on Coupled Dark Energy from the Planck satellite experiment, *Phys. Rev. D* **88**, 023531 (2013), arXiv:1304.7119 [astro-ph.CO].
- [223] C. Caprini and N. Tamanini, Constraining early and interacting dark energy with gravitational wave standard sirens: the potential of the eLISA mission, *JCAP* **10**, 006, arXiv:1607.08755 [astro-ph.CO].
- [224] X. Zheng, M. Biesiada, S. Cao, J. Qi, and Z.-H. Zhu, Ultra-compact structure in radio quasars as a cosmological probe: a revised study of the interaction between cosmic dark sectors, *JCAP* **10**, 030, arXiv:1705.06204 [astro-ph.CO].
- [225] J. Zhang, R. An, W. Luo, Z. Li, S. Liao, and B. Wang, The First Constraint from SDSS Galaxy–Galaxy Weak Lensing Measurements on Interacting Dark Energy Models, *Astrophys. J. Lett.* **875**, L11 (2019), arXiv:1807.05522 [astro-ph.CO].
- [226] L. Xiao, A. A. Costa, and B. Wang, Forecasts on interacting dark energy from the 21-cm angular power spectrum with BINGO and SKA observations, *Mon. Not. Roy. Astron. Soc.* **510**, 1495 (2021), arXiv:2103.01796 [astro-ph.CO].
- [227] A. Joseph and R. Saha, Forecast analysis on interacting dark energy models from future generation PICO and DESI missions, *Mon. Not. Roy. Astron. Soc.* **519**, 1809 (2022), arXiv:2209.07167 [astro-ph.CO].
- [228] U. Mukhopadhyay, D. Majumdar, and K. K. Datta, Probing interacting dark energy and scattering of baryons with dark matter in light of the EDGES 21-cm signal, *Phys. Rev. D* **103**, 063510 (2021), arXiv:2008.09972 [astro-ph.CO].
- [229] Y. Zhao, Y. Liu, S. Liao, J. Zhang, X. Liu, and W. Du, Constraining interacting dark energy models with the halo concentration–mass relation, *Mon. Not. Roy. Astron. Soc.* **523**, 5962 (2023), arXiv:2212.02050 [astro-ph.CO].
- [230] A. A. Costa, X.-D. Xu, B. Wang, E. G. M. Ferreira, and E. Abdalla, Testing the Interaction between Dark Energy and Dark Matter with Planck Data, *Phys. Rev. D* **89**, 103531 (2014), arXiv:1311.7380 [astro-ph.CO].
- [231] A. A. Costa, X.-D. Xu, B. Wang, and E. Abdalla, Constraints on interacting dark energy models from Planck 2015 and redshift-space distortion data, *JCAP* **01**, 028, arXiv:1605.04138 [astro-ph.CO].
- [232] R. An, C. Feng, and B. Wang, Constraints on the dark matter and dark energy interactions from weak lensing bispectrum tomography, *JCAP* **10**, 049, arXiv:1706.02845 [astro-ph.CO].
- [233] R. An, C. Feng, and B. Wang, Relieving the Tension between Weak Lensing and Cosmic Microwave Background with Interacting Dark Matter and Dark Energy Models, *JCAP* **02**, 038, arXiv:1711.06799 [astro-ph.CO].
- [234] R. R. A. Bachega, A. A. Costa, E. Abdalla, and K. S. F. Fornasier, Forecasting the Interaction in Dark Matter–Dark Energy Models with Standard Sirens From the Einstein Telescope, *JCAP* **05**, 021, arXiv:1906.08909 [astro-ph.CO].
- [235] C. Li, X. Ren, M. Khurshudyan, and Y.-F. Cai, Implications of the possible 21-cm line excess at cosmic dawn on dynamics of interacting dark energy, *Phys. Lett. B* **801**, 135141 (2020), arXiv:1904.02458 [astro-ph.CO].
- [236] A. Halder and M. Pandey, Probing the effects of primordial black holes on 21-cm EDGES signal along with interacting dark energy and dark matter–baryon scattering, *Mon. Not. Roy. Astron. Soc.* **508**, 3446 (2021), arXiv:2101.05228 [astro-ph.CO].
- [237] M. Aljaf, D. Gregoris, and M. Khurshudyan, Constraints on interacting dark energy models through cosmic chronometers and Gaussian process, *Eur. Phys. J. C* **81**, 544 (2021), arXiv:2005.01891 [astro-ph.CO].
- [238] M. Califano, I. De Martino, and R. Lazkoz, Probing interacting dark sector with the next generation of gravitational-wave detectors, *Phys. Rev. D* **110**, 083519 (2024), arXiv:2410.06152 [gr-qc].
- [239] S. Pan, W. Yang, C. Singha, and E. N. Saridakis, Observational constraints on sign-changeable interaction models and alleviation of the H_0 tension, *Phys. Rev. D* **100**, 083539 (2019), arXiv:1903.10969 [astro-ph.CO].
- [240] H.-L. Li, J.-F. Zhang, and X. Zhang, Constraints on neutrino mass in the scenario of vacuum energy interacting with cold dark matter after Planck 2018, *Commun. Theor. Phys.* **72**, 125401 (2020), arXiv:2005.12041 [astro-ph.CO].
- [241] R.-Y. Guo, L. Feng, T.-Y. Yao, and X.-Y. Chen, Exploration of interacting dynamical dark energy model with interaction term including the equation-of-state parameter: alleviation of the H_0 tension, *JCAP* **12** (12), 036, arXiv:2110.02536 [gr-qc].
- [242] L.-F. Wang, J.-H. Zhang, D.-Z. He, J.-F. Zhang, and X. Zhang, Constraints on interacting dark energy models from time-delay cosmography with seven lensed quasars, *Mon. Not. Roy. Astron. Soc.* **514**, 1433 (2022), arXiv:2102.09331 [astro-ph.CO].

- [243] L. Santos, W. Zhao, E. G. M. Ferreira, and J. Quintin, Constraining interacting dark energy with CMB and BAO future surveys, *Phys. Rev. D* **96**, 103529 (2017), arXiv:1707.06827 [astro-ph.CO].
- [244] D. Grandon and V. H. Cardenas, Exploring evidence of interaction between dark energy and dark matter (2018), arXiv:1804.03296 [astro-ph.CO].
- [245] R. von Marttens, L. Casarini, D. F. Mota, and W. Zimdahl, Cosmological constraints on parametrized interacting dark energy, *Phys. Dark Univ.* **23**, 100248 (2019), arXiv:1807.11380 [astro-ph.CO].
- [246] H. Yan, Y. Pan, J.-X. Wang, W.-X. Xu, and Z.-H. Peng, Investigating interacting dark energy models using fast radio burst observations*, *Chin. Phys.* **49**, 115109 (2025), arXiv:2507.16308 [astro-ph.CO].
- [247] R. Nagpal, A. Kandel, R. Mandal, U. Debnath, and S. K. J. Pacif, SSFDE Model: Cosmological Implications and Dynamical System Analysis, arXiv preprint (2025), arXiv:2511.06129 [gr-qc].
- [248] W. Yang, S. Pan, R. C. Nunes, and D. F. Mota, Dark calling Dark: Interaction in the dark sector in presence of neutrino properties after Planck CMB final release, *JCAP* **04**, 008, arXiv:1910.08821 [astro-ph.CO].
- [249] E. Di Valentino, A. Melchiorri, O. Mena, and S. Vagnozzi, Nonminimal dark sector physics and cosmological tensions, *Phys. Rev. D* **101**, 063502 (2020), arXiv:1910.09853 [astro-ph.CO].
- [250] W. Yang, S. Pan, O. Mena, and E. Di Valentino, On the dynamics of a dark sector coupling, *JHEAp* **40**, 19 (2023), arXiv:2209.14816 [astro-ph.CO].
- [251] T. Clemson, K. Koyama, G.-B. Zhao, R. Maartens, and J. Valiviita, Interacting Dark Energy – constraints and degeneracies, *Phys. Rev. D* **85**, 043007 (2012), arXiv:1109.6234 [astro-ph.CO].
- [252] R. C. Nunes, S. Vagnozzi, S. Kumar, E. Di Valentino, and O. Mena, New tests of dark sector interactions from the full-shape galaxy power spectrum, *Phys. Rev. D* **105**, 123506 (2022), arXiv:2203.08093 [astro-ph.CO].
- [253] F. Arevalo, A. P. R. Bacalhau, and W. Zimdahl, Cosmological dynamics with non-linear interactions, *Class. Quant. Grav.* **29**, 235001 (2012), arXiv:1112.5095 [astro-ph.CO].
- [254] J.-H. He and B. Wang, Effects of the interaction between dark energy and dark matter on cosmological parameters, *JCAP* **06**, 010, arXiv:0801.4233 [astro-ph].
- [255] J. S. Lima, R. von Marttens, and L. Casarini, Interacting dark sector with quadratic coupling: theoretical and observational viability, *Eur. Phys. J. Plus* **140**, 297 (2025), arXiv:2412.16299 [astro-ph.CO].
- [256] S. M. Carroll, M. Hoffman, and M. Trodden, Can the dark energy equation of state parameter w be less than -1?, *Phys. Rev. D* **68**, 023509 (2003), arXiv:astro-ph/0301273.
- [257] J. Santos, J. S. Alcaniz, N. Pires, and M. J. Reboucas, Energy Conditions and Cosmic Acceleration, *Phys. Rev. D* **75**, 083523 (2007), arXiv:astro-ph/0702728.
- [258] V. A. Rubakov, The Null Energy Condition and its violation, *Phys. Usp.* **57**, 128 (2014), arXiv:1401.4024 [hep-th].
- [259] P. Martin-Moruno and M. Visser, Classical and semi-classical energy conditions, *Fundam. Theor. Phys.* **189**, 193 (2017), arXiv:1702.05915 [gr-qc].
- [260] J. Valiviita, R. Maartens, and E. Majerotto, Observational constraints on an interacting dark energy model, *Mon. Not. Roy. Astron. Soc.* **402**, 2355 (2010), arXiv:0907.4987 [astro-ph.CO].
- [261] T. Delubac *et al.* (BOSS), Baryon acoustic oscillations in the Ly α forest of BOSS DR11 quasars, *Astron. Astrophys.* **574**, A59 (2015), arXiv:1404.1801 [astro-ph.CO].
- [262] V. Poulin, K. K. Boddy, S. Bird, and M. Kamionkowski, Implications of an extended dark energy cosmology with massive neutrinos for cosmological tensions, *Phys. Rev. D* **97**, 123504 (2018), arXiv:1803.02474 [astro-ph.CO].
- [263] Y. Wang, L. Pogosian, G.-B. Zhao, and A. Zucca, Evolution of dark energy reconstructed from the latest observations, *Astrophys. J. Lett.* **869**, L8 (2018), arXiv:1807.03772 [astro-ph.CO].
- [264] L. Visinelli, S. Vagnozzi, and U. Danielsson, Revisiting a negative cosmological constant from low-redshift data, *Symmetry* **11**, 1035 (2019), arXiv:1907.07953 [astro-ph.CO].
- [265] R. Calderón, R. Gannouji, B. L'Huillier, and D. Polarski, Negative cosmological constant in the dark sector?, *Phys. Rev. D* **103**, 023526 (2021), arXiv:2008.10237 [astro-ph.CO].
- [266] Y. C. Ong, An Effective Sign Switching Dark Energy: Lotka–Volterra Model of Two Interacting Fluids, *Universe* **9**, 437 (2023), arXiv:2212.04429 [gr-qc].
- [267] M. Malekjani, R. M. Conville, E. Ó. Colgáin, S. Pourojaghi, and M. M. Sheikh-Jabbari, On redshift evolution and negative dark energy density in Pantheon + Supernovae, *Eur. Phys. J. C* **84**, 317 (2024), arXiv:2301.12725 [astro-ph.CO].
- [268] M. Bouhmadi-López and B. Ibarra-Uriondo, Cosmological perturbations for smooth sign-switching dark energy models (2025), arXiv:2506.18992 [gr-qc].
- [269] A. Gómez-Valent and A. González-Fuentes, Effective Phantom Divide Crossing with Standard and Negative Quintessence (2025), arXiv:2508.00621 [astro-ph.CO].
- [270] A. González-Fuentes and A. Gómez-Valent, Reconstruction of dark energy and late-time cosmic expansion using the Weighted Function Regression method (2025), arXiv:2506.11758 [astro-ph.CO].
- [271] P. Ghafari, M. Najafi, M. Ghodsi Yengejeh, E. Özilker, E. Di Valentino, and J. T. Firouzjaee, A Multi-Probe ISW Study of Dark Energy Models with Negative Energy Density: Galaxy Correlations, Lensing Bispectrum, and Planck ISW-Lensing Likelihood (2025), arXiv:2512.07060 [astro-ph.CO].
- [272] M. B. Gavela, D. Hernandez, L. Lopez Honorez, O. Mena, and S. Rigolin, Dark coupling, *JCAP* **07**, 034, [Erratum: *JCAP* **05**, E01 (2010)], arXiv:0901.1611 [astro-ph.CO].
- [273] W. Yang, S. Pan, E. Di Valentino, O. Mena, and A. Melchiorri, 2021-H0 odyssey: closed, phantom and interacting dark energy cosmologies, *JCAP* **10**, 008, arXiv:2101.03129 [astro-ph.CO].
- [274] Y.-H. Li, J.-F. Zhang, and X. Zhang, Parametrized Post-Friedmann Framework for Interacting Dark Energy, *Phys. Rev. D* **90**, 063005 (2014), arXiv:1404.5220 [astro-ph.CO].

- [275] Y.-H. Li, J.-F. Zhang, and X. Zhang, Exploring the full parameter space for an interacting dark energy model with recent observations including redshift-space distortions: Application of the parametrized post-Friedmann approach, *Phys. Rev. D* **90**, 123007 (2014), arXiv:1409.7205 [astro-ph.CO].
- [276] C. Skordis, A. Pourtsidou, and E. J. Copeland, Parametrized post-Friedmannian framework for interacting dark energy theories, *Phys. Rev. D* **91**, 083537 (2015), arXiv:1502.07297 [astro-ph.CO].
- [277] X. Zhang, Probing the interaction between dark energy and dark matter with the parametrized post-Friedmann approach, *Sci. China Phys. Mech. Astron.* **60**, 050431 (2017), arXiv:1702.04564 [astro-ph.CO].
- [278] L. Feng, Y.-H. Li, F. Yu, J.-F. Zhang, and X. Zhang, Exploring interacting holographic dark energy in a perturbed universe with parameterized post-Friedmann approach, *Eur. Phys. J. C* **78**, 865 (2018), arXiv:1807.03022 [astro-ph.CO].
- [279] J.-P. Dai and J. Xia, Revisiting the Instability Problem of the Interacting Dark Energy Model in the Parameterized Post-Friedmann Framework, *Astrophys. J.* **876**, 125 (2019), arXiv:1904.04149 [astro-ph.CO].
- [280] Y.-H. Li and X. Zhang, IDECAMB: an implementation of interacting dark energy cosmology in CAMB, *JCAP* **09**, 046, arXiv:2306.01593 [astro-ph.CO].
- [281] E. Silva, G. Hartmann, and R. C. Nunes, One-loop power spectrum corrections in interacting dark energy cosmologies (2025), arXiv:2512.11678 [astro-ph.CO].
- [282] T. Brinckmann and J. Lesgourgues, MontePython 3: boosted MCMC sampler and other features, *Phys. Dark Univ.* **24**, 100260 (2019), arXiv:1804.07261 [astro-ph.CO].
- [283] B. Audren, J. Lesgourgues, K. Benabed, and S. Prunet, Conservative Constraints on Early Cosmology: an illustration of the Monte Python cosmological parameter inference code, *JCAP* **02**, 001, arXiv:1210.7183 [astro-ph.CO].
- [284] D. Blas, J. Lesgourgues, and T. Tram, The Cosmic Linear Anisotropy Solving System (CLASS) II: Approximation schemes, *JCAP* **07**, 034, arXiv:1104.2933 [astro-ph.CO].
- [285] M. Moresco, Measuring the expansion history of the Universe with cosmic chronometers, arXiv preprint (2024), arXiv:2412.01994 [astro-ph.CO].
- [286] N. Schöneberg, The 2024 BBN baryon abundance update, *JCAP* **06**, 006, arXiv:2401.15054 [astro-ph.CO].
- [287] A.-K. Burns, T. M. P. Tait, and M. Valli, PRyMordial: the first three minutes, within and beyond the standard model, *Eur. Phys. J. C* **84**, 86 (2024), arXiv:2307.07061 [hep-ph].
- [288] H. Akaike, A new look at the statistical model identification, *IEEE Trans. Automatic Control* **19**, 716 (1974).
- [289] X. Zhang, F.-Q. Wu, and J. Zhang, A New generalized Chaplygin gas as a scheme for unification of dark energy and dark matter, *JCAP* **01**, 003, arXiv:astro-ph/0411221.
- [290] R. Kou and A. Lewis, Unified dark fluid with null sound speed as an alternative to phantom dark energy (2025), arXiv:2509.16155 [astro-ph.CO].
- [291] G. Aguilar-Pérez, M. Cruz, M. Fathi, and J. R. Villanueva, Interacting Generalized Chaplygin-Jacobi gas: Thermodynamics approach (2025), arXiv:2512.02900 [gr-qc].